POLYMER MEDIATED PROTEIN CRYSTALLISATION

DIMITRA NIKOLAIDI, BSc.

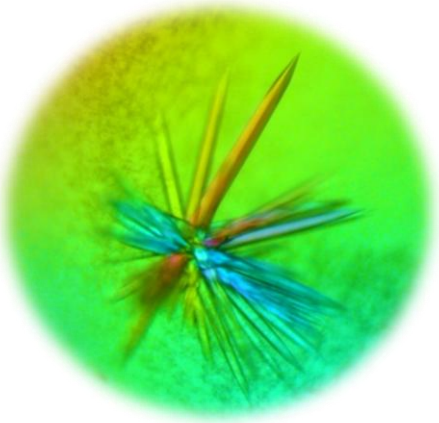

Thesis submitted to the University of Nottingham
for the degree of Master of Philosophy

July 2013

ABSTRACT

Structure elucidation of a macromolecule can lead to the determination of its function. In the case of proteins, knowledge of their three-dimensional structure can be utilised in the identification of active site(s) and consequently in rational drug design. Commonly, X-ray crystallography is implemented on a high quality single crystal of the target macromolecule, in order to elucidate its structure. Moreover, crystallised protein molecules may remain active which can then be used in controlled drug delivery. Unfortunately, the successful crystallisation of a macromolecule can be seen as the most challenging aspect in this endeavour, given that predicting, screening and directing crystallisation remains an elusive goal.

A possible solution to this problem is the use of heterogeneous nucleation, where a foreign surface is employed to lower the energy barrier for nucleation to occur. Heteronucleation has been utilised in the crystallisation of small organic molecules, inorganic complexes, extended networks and proteins. Polymeric surfaces, as heteronucleants, in protein crystallisation have been known to increase nucleation density rates and selectively crystallise particular forms of proteins. Moreover, imprinted polymeric surfaces have been successfully used to selectively crystallise inorganic molecules as well as a small range of well studied proteins.

This thesis presents the effects of polymers on the crystallisation of two proteins, that of mutant human thioredoxin and wild-type hen egg-white lysozyme (HEWL). Polymers were used in solution, as physically adsorbed films as well as plasma polymers. Shape and size of the protein crystals was altered, while polymorphism was also achieved, in the presence of polymers with various functionalities. This work is a step towards the use of polymers as heteronucleants in directing protein crystallisation.

ACKNOWLEDGEMENTS

I would like to offer my thanks to Professor Cameron Alexander, Professor Morgan Alexander, Dr Cristina De Matteis and Dr Jonas Emsley for their help and advice during the past years. Funding for this project from the BBSRC is also gratefully acknowledged.

I wish to thank Dr Elizabeth Hooley for all her help, patience and expertise in the area of crystallisation, and Dr Gareth Hall for kindly providing purified human thioredoxin protein for crystallisation. Professor Xinyong Chen and Dr Emily Smith are acknowledged for Atomic Force Microscopy (AFM) and X-ray Photoelectron Spectroscopy (XPS) training and help with data acquisition respectively. I also wish to thank Dr David Scurr and Dr Paul McEwan for many useful discussions.

I would like to express my thanks to Mrs Christine Grainger-Boultby and Mr Paul Cooling who were invaluable to keep the laboratories running and to Mr Richard Johnson, Mrs Julia Crouch and Mrs Gail Atkinson for all their help in administrative work.

I also want to acknowledge Mrs Lynne McDermott, Dr Hugh Porter, Professor Clive Adams, Claire Thompson, part of the Cripps Health Centre team, and especially Dr Lisa Rull, of the University of Nottingham Academic Support team, for all their help, encouragement and advice these last few years and for giving me enough strength to complete this work.

I wish to thank from the bottom of my heart all my friends and colleagues in D19 and D20, especially Emilia, Mathieu, Driton, Declan, Sam, Abdennour, Vladimir and Sabrina, for their company and support which proved invaluable during this work.

Many thanks go to Olympia and Anwar, for being great friends through all the good times and even greater friends through all the difficult times. I also wish to thank my best friend Nina for being so understanding and always willing to listen to a friend in need.

To my mum and dad for giving me the opportunity to go after my dreams, for supporting my decisions and always having my best interests at heart, I shall always be thankful and grateful to have you as my parents.

Last but by no means least; to my sister I wish to give the greatest thanks. She has been my friend, my mother, my father, my world and nothing shall ever be enough to show how much she means to me. This, Rika is for you.

TABLE OF CONTENTS

LIST OF FIGURES

LIST OF TABLES

ABBREVIATIONS

°	Degree(s)
Å	Angstrom
°C	Degree(s) Celsius
θ	Contact angle
AFM	Atomic force microscopy
CML	Chronic myelogenous leukaemia
E.C.	Enzyme commission (number)
eV	Electron volt
FAT	Fixed analyser transmission
h	Hour(s)
HEWL	Hen egg-white lysozyme
H_2O	Water
kDa	Kilodalton(s)
µm	Micrometre(s) (=10^{-6} metre(s))
µl	Microlitre(s) (=10^{-6} litre(s))
M	Molar
MeOH	Methanol
min	Minute(s)
mg	Milligram(s) (=10^{-3} gram(s))

ml	Millilitre(s) (=10^{-3} litre(s))
mM	Millimolar (=10^{-3} molar)
mTorr	Millitorr (=10^{-3} torr)
Mv	Viscosity average molecular weight
Mw	Weight average molecular weight
MΩ	Megaohm(s) (=10^{6} ohm(s))
NaCl	Sodium chloride
NADPH	Reduced form of nicotinamide adenine dinucleotide phosphate
NB	Nota bene (note well)
nm	Nanometre(s) (=10^{-9} metre(s)
NMR	Nuclear magnetic resonance
PAA	Polyacrylic acid
PAAm	Polyallylamine
PDB	Protein data bank
PEG 300	Polyethylene glycol Mw ~300
pI	Isoelectric point
ppAA	Plasma polymerised acrylic acid
ppAAm	Plasma polymerised allylamine
ppAOH	Plasma polymerised allyl alcohol
PVOH	Polyvinyl alcohol

PVP	Polyvinyl pyrrolidone
rpm	Revolutions per minute
RT	Room temperature
TRIS-HCl	Tris(hydroxymethyl)aminomethane hydrochloride
UHV	Ultra high vacuum
v/v	Volume/volume
W	Watt(s)
w/v	Weight/volume
WCA	Water contact angle
XPS	X-ray photoelectron spectroscopy

CHAPTER 1

1. Introduction

1.1. Prologue

This chapter introduces the aim of this work and defines its objectives. To set the scene of the research this chapter will cover crystallisation, its basic principles, various techniques of crystallisation, challenges that have risen thus far, as well as research conducted in predicting and controlling crystallisation. It will explain why there is a need to crystallise proteins, and focus on polymers and their uses in protein crystallisation. Furthermore, the premise of the research will be presented and the proteins utilised in the thesis will be introduced.

1.2. Why Crystallise Proteins?

The three-dimensional structure of a biological macromolecule (nucleic acid, protein, virus) can play a vital role towards understanding the function of said macromolecule.

In the case of proteins, these polypeptides are formed out of 20 naturally occurring amino acid residues which are covalently linked via peptide bonds to form the primary structure of each protein. The chemical properties of the amino acids (hydrophilicity, hydrophobicity, charged, uncharged) that comprise a protein determine how these residues interact with one another within the protein. Protein structure is primarily driven by the non-covalent interactions of the protein residues. Hydrogen bonding between the residues of the protein stabilise the formation of sub-structures, such as alpha (α-) helices and beta (β-) sheets, which give rise to the secondary structure of a protein.

The tertiary structure of a protein refers to its final three-dimensional structure, where the secondary structures are folded further, driven by several non-covalent interactions, such as hydrogen bonding, hydrophobic interactions, electrostatic interactions and Van der Walls forces. The domains formed by these interactions can be further stabilised by salt bridges and/or covalent disulphide bonds. Moreover, certain proteins, such as haemoglobin, have a quaternary structure which is formed when two or more polypeptides interact to form the final protein structure. The polypeptides that comprise quaternary structured proteins can be identical or different subunits which are then stabilised by the same non-covalent interactions as those giving rise to the tertiary protein structure, as well as disulphide bridges. The complexity of the three-dimensional structure of a protein is illustrated in Figure 1.1.

The folding of amino acid residue chains and the formation of the three-dimensional structure of a protein needs to be elucidated in order to identify active site(s), possible areas of interactions with other (macro)molecules, or similarities in structure with other known proteins, which can lead to function elucidation. While there are crystal structure prediction software, such as I-TASSER, that can be used to predict the possible structure and function of a protein based on its primary structure, the software results are not 100% reliable.

Nuclear magnetic resonance (NMR) spectroscopy can be employed to determine the three-dimensional structures of proteins. Solution NMR is usually limited in the structural elucidation of small proteins (≤35 kDa), due to the complexity of the NMR spectra produced by larger proteins. However, recent advances have led to the structural elucidation of large proteins, such as the 900 kDa bacterial chaperone complex GroEL-GroES (1). An advantage of solution NMR is that it provides data consistent with

a number of possible structures for the same protein, which in turn provide a more dynamic view of the protein structure.

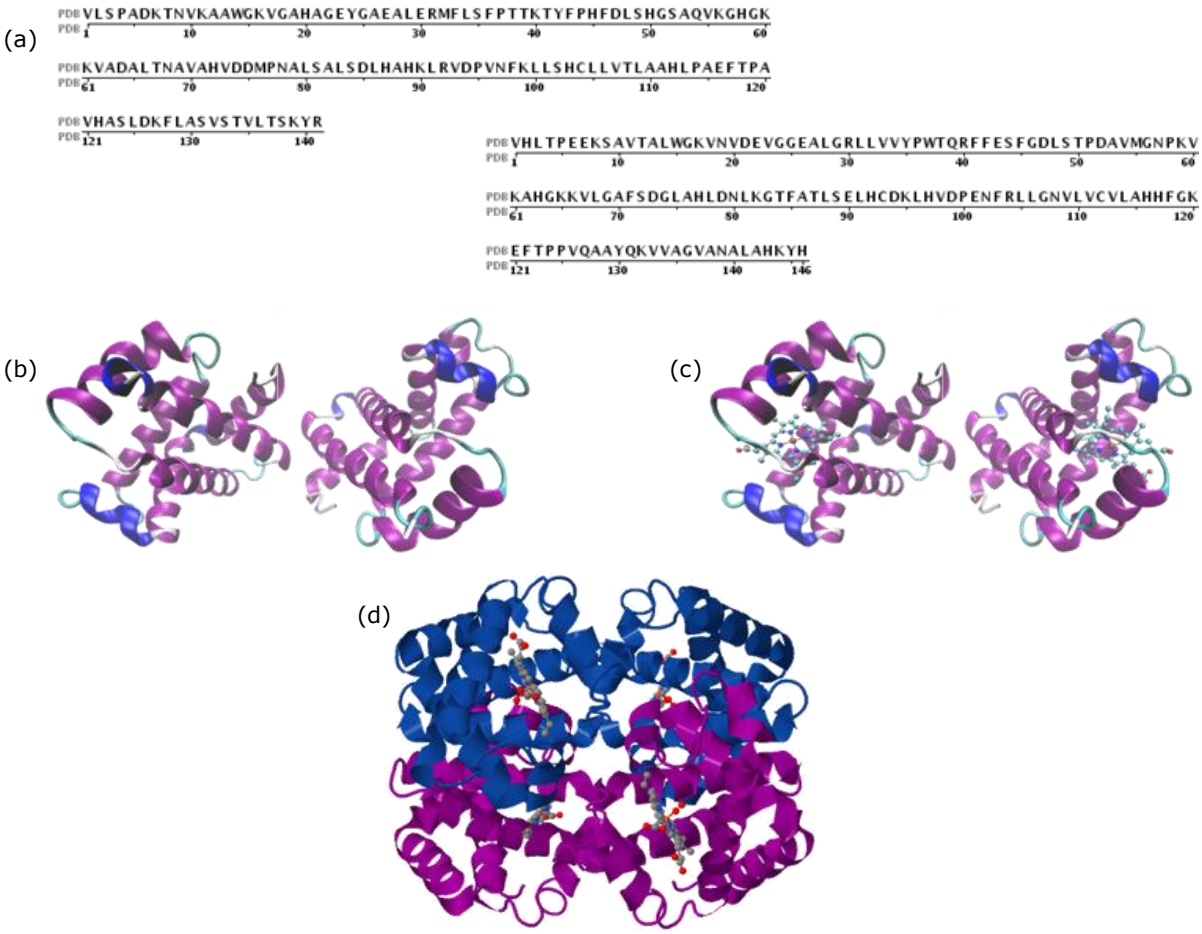

Figure 1.1. Schematic representation illustrating the structural complexity of proteins, using human haemoglobin as an example. Haemoglobin is a tetrameric globular protein comprised of two α and two β subunits. The (a) primary structure of haemoglobin consists of the 141 and 146 amino acid sequence of the α and β subunits respectively. The (b) secondary, (c) tertiary and (d) quaternary structure of haemoglobin is also depicted. The quaternary structure of the protein was determined by B. Shaanan using X-ray crystallography (2).

The most common method for protein structure elucidation is X-ray crystallography (3) and accounts for 87% of the structures deposited in the Protein Data Bank (PDB) (4). The target protein must undergo crystallisation in order to afford a high quality large single crystal. X-ray crystallography is then employed and a diffraction pattern of the crystal is obtained, which is used to elucidate the protein structure. In comparison to solution NMR, a single protein structure is obtained, which gives a more

static view of the protein structure. However, X-ray crystallography is not limited by the size of the protein. Synchrotron X-ray sources, like the Diamond Light Source in Oxfordshire, can analyse small crystals (≤10 μm in all dimensions), while conventional X-ray sources can analyse larger crystals (50–250 μm in all dimensions) (5).

Once the native structure (i.e. natural, unaltered structure) of a protein is known, rational drug design can also be employed. For example, in diseases such as cancer, certain biological pathways can be activated by particular proteins. Knowledge of the three-dimensional structure of those proteins can be used in rational drug design, resulting in the synthesis of drug molecules that are designed to fit and bind into the active site(s) of the target proteins, thus blocking protein function. A successful example of structure-based rational drug design is imatinib, marketed as Glivec (Europe) or Gleevec (USA). It was designed specifically as an inhibitor to the *bcr-abl* fusion protein, which is a tyrosine kinase, caused by a chromosomal translocation (the Philadelphia chromosome) found in chronic myelogenous leukaemia (CML). As imatinib targets this specific tyrosine kinase fusion protein, it is able to target selectively the cancer cells of the patient (6).

Aside from structure/function elucidation and rational drug design, protein crystallisation is also important in controlled drug delivery. Drug levels in a human organism cannot be sustained over a prolonged period of time, due to the body's metabolism. In order to confirm that crystallised protein macromolecules have remained in active form within the crystal lattice, activity assays can be utilised. The non-covalent bonds that connect the crystallised protein molecules can then be broken resulting in individual active protein macromolecules. Thus, drugs that are proteins, such as insulin, in the form of crystals show promise in controlled delivery, when

encapsulated within biodegradable polymer shells, which serve to protect the protein and allow for controlled drug release (7). Uniform sized crystals are required for the dosing to be reproducible, when using crystallised proteins as drugs.

Therefore, protein crystallisation can be utilised for structure/function elucidation, rational drug design as well as controlled drug delivery. Since the first protein crystallisation, that of earthworm haemoglobin in 1840 by Hünefeld, to today, protein crystallisation is proving a challenging area of research. While there are attempts at using bioinformatics in order to predict whether a protein can crystallise (8), the successful prediction and control of protein crystallisation remains elusive mainly due to the fact that every protein has a unique three-dimensional structure with different surface characteristics. Moreover, difficulties in extracting and purifying the target protein (prior to crystallisation), problems with protein solubility or even the limited amount of protein purified (once extracted from samples), are frequently encountered.

There are commercial screening kits (9) available that offer a variety of crystallisation conditions, by varying in salts, buffers and precipitants. Use of such kits can lead to the identification of suitable salt/buffer/precipitant conditions for the successful crystallisation of a particular protein. Subtle changes in the crystallisation conditions may afford different crystal forms of the target macromolecule.

1.3. Basic Principles of Crystallisation

The word ‘crystal’, derived from the Greek word ‘κρύσταλλος’ meaning clear ice, is used to describe a homogeneous solid that is formed by an orderly three-dimensional array of atoms, ions, molecules, or molecular

assemblies held together by non-covalent interactions. Single crystals appear transparent and can have distinct geometrical crystal classes (triclinic, monoclinic, orthorhombic, tetragonal, rhombohedral, hexagonal, cubic), with regular faces and well-defined edges (Table 1.1).

Crystal System Crystals get grouped in one of the seven crystal systems according to the three types of symmetry: plane, axis and centre of symmetry	**Plane of Symmetry** Represents an imaginary plane through the centre of the crystal dividing the crystal into two halves, both being mirror images of each other (10)	**Axis of Symmetry** Represents an imaginary line through the centre of a crystal so that the rotation of the crystal about this line results in the arrangement of faces and angles being identical with that of the starting position (10)	**Centre of Symmetry** The point at which all the axes meet and through which the planes of symmetry pass (10)
Triclinic	0	0 axes	1 or 0
Monoclinic	1	1 two-fold axis	1
Orthorhombic	3	3 two-fold axes mutually perpendicular	1
Tetragonal	5	1 four-fold axis	1
Rhombohedral	3	1 three-fold axis	1
Hexagonal	7	1 six-fold axis	1
Cubic	9	minimum of 4 three-fold axes	1

Table 1.1. Table showing the seven crystal systems and the three types of symmetry used to categorise crystal structures: plane, axis and centre of symmetry (11). The crystal systems are presented in order of least to most symmetric.

Crystallisation is the process by which crystals are formed in three stages: nucleation, growth of crystal(s) and termination of crystal growth. Crystals can be formed from solutions, melts and gases. Crystallisation is a reversible equilibrium phenomenon, driven by the minimisation of the system's free energy (12). To crystallise solute molecules from a solution, it is necessary for the molecules to be at a supersaturated state. In a supersaturated solution there is such an increased amount of solute molecules that they are not fully solvated. A supersaturated solution is a

chemical system that is not at equilibrium. The system is thermodynamically driven to a new equilibrium state with a new free energy minimum, where solute molecules are driven out of solution and into the solid state. Aggregation of solute molecules, and formation of non-covalent bonds between them, minimises the free energy of the system. Thus, due to kinetics, nucleation is most practically achieved at higher levels of supersaturation than those used for crystal growth.

Nuclei formation is affected by diffusion and convection. Convection currents are formed as regions near the growing crystal have a lower crystallising molecule concentration than the rest of the solution, resulting in the formation of density gradients (13). Crystallising solute molecules, at a supersaturated state, have a higher energy than solutes in a crystalline state. In order to reach the crystalline state a critical nucleus must be formed, which has a higher energy than the free solute molecules. This is the energy barrier that must be overcome prior to crystal formation. The speed at which the critical nuclei appear, determines the rate at which nucleation occurs (14).

Nuclei are unstable and can spontaneously dissolve unless they reach 'critical size', which is determined by the ratio between surface area of the nucleus and its volume (15). Once stable nuclei are formed they can grow further to form crystals. Studies have shown that the rate of crystal growth is constant in a supersaturated solution, until termination of crystal growth occurs, provided that all other variables, such as temperature, remain constant (16).

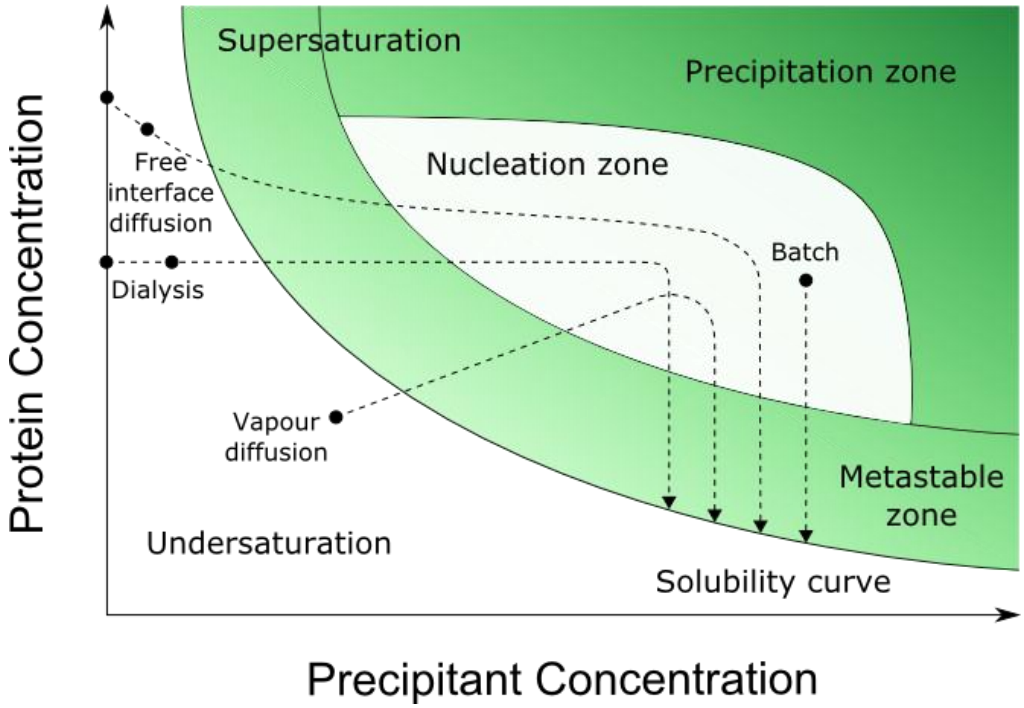

Figure 1.2. Schematic drawing of a protein crystallisation phase diagram based on two of the most commonly varied parameters, protein and precipitant concentrations. The four major crystallisation methods are highlighted showing that in order to produce crystals, all the systems need to reach the same destination, namely the nucleation zone, after which they make their way through the metastable zone and eventually arrive at the solubility curve. Each method achieves this journey via a different route. The black dots (•) represent the starting conditions. In the case of dialysis and free-interface diffusion two alternative starting points are shown since the undersaturated protein solution can contain solely protein or alternatively, protein with a low concentration of the precipitating agents (17).

Figure 1.2 is a typical crystallisation phase diagram. The undersaturation zone is where most vapour and liquid diffusion crystallisation experiments start. The types of crystallisation experiments are explained further in section 1.4. There are four zones of supersaturation; the precipitation zone is the highest supersaturation zone where proteins have random intermolecular interactions at a faster rate and as a result amorphous precipitate forms. The nucleation (labile) zone is of moderate supersaturation and under those conditions ordered, periodical intermolecular interactions take place at a slower rate and may result in the formation of crystal nuclei (18). The metastable zone is a lower supersaturation phase where the conditions observed are ideal for the growth of well-ordered crystals. At the metastable zone no crystal

nucleation may take place (19). The end point of a crystallisation experiment is the solubility curve, which is a dynamic equilibrium where the crystal is stable.

Crystal growth is terminated either due to concentration decrease of the crystallising solute (towards reaching equilibrium), or due to the fact that the crystal has reached a certain size and cannot grow further. The time required for large single crystals to form can vary from a few days to several months (20).

Incorporation of impurities or damaged crystallising solute molecules, in the growing face of a crystal, leads to interruption of the growing crystal lattice. This is called 'poisoning' of the crystal, and the caused disruption in the internal order of the crystal, over many atomic dimensions, can lead to the loss of crystalline properties, such as shape, regular faces and well-defined edges (18).

Inorganic compounds, such as minerals, as well as organic compounds, such as sugars and proteins, can be crystallised under certain conditions. Subtle changes in the crystallisation conditions can alter the relative arrangement of the crystallising molecules within the crystal, resulting in crystals that belong to different crystal systems. The various crystal forms arising from the same crystallising molecule are called polymorphs, of said compound. Polymorphs have different physical properties, such as crystal habit (i.e. crystal size and shape), melting point and dissolution rate. Thus, under patent law, a new crystal form of a compound can be considered as an innovation. An example of polymorphism can be seen in acetaminophen, which has three polymorphs: monoclinic (form I), orthorhombic (form II) and form III which is a metastable bilayer structure (21, 22). In the case of proteins, the term forms, and not

polymorphs, is used since each protein crystal form has a unique composition arising from variable water content and buffer components.

While supersaturation of the system drives both nucleation and crystal growth, the rate of nucleation differs from the crystal growth rate. Both rates can affect the habit of the crystal (i.e. shape and size) as well as crystal quality. Multiple crystal nuclei and a fast crystal growth rate can result in the formation of numerous microcrystals. Few crystal nuclei and a slow crystal growth rate usually results in large, single crystals, which are more desirable for single crystal X-ray crystallography analysis. Moreover, altering the rates of nucleation and crystal growth may result in the formation of a different crystal polymorph/form (23).

Other factors which affect protein crystallisation include purity of the protein sample, temperature, pH and precipitant type. A common precipitant is salt (NaCl), which can compete with protein molecules for solvent molecules, resulting in a 'salting out' effect, as protein molecules are forced to self-associate in order to fulfil their electrostatic requirements. Crystallisation pH is chosen according to the optimum pH range of the protein (so as not to denature it) and taking into consideration the isoelectric point of the protein (pI).

Temperature is an important factor in protein crystallisation and should be maintained within ±1°C in order to achieve replicable and reliable results; unless temperature variation is desired in the experiment. As the solubility of proteins is temperature dependant, and could decrease or increase depending on the target protein, crystallisation usually takes place between 4°C to 19°C and can even reach 35°C with the use of incubators, which are set at a constant temperature (24). Temperature affects the kinetics of crystallisation. For example, if low temperatures

decrease the solubility of a specific protein, they can lead to supersaturation but also decrease diffusion, due to low kinetics, resulting in slow crystal growth. Experiments conducted on porcine pancreatic α-amylase demonstrated that the growth rate of A_I and B_{II} crystal forms increased dramatically when temperature was increased above 18°C (25).

As for protein sample purity, it is paramount in order to grow a high quality single crystal without impurities 'poisoning' the crystal during its formation. Ligands, such as drugs, can sometimes be added to a protein sample, in order to stabilise the conformation of the protein and allow for crystallisation to take place.

1.4. Crystallisation Techniques

There are various crystallisation techniques, the three most popular, in descending order of popularity, are vapour diffusion, batch and dialysis (26). Each of these techniques should achieve supersaturation by the slow increase in concentration of some precipitant, such as salt or polyethylene glycol (PEG) (Figure 1.2). During use of these techniques other factors can also be altered, such as pH and temperature.

1.4.1. Vapour Diffusion Crystallisation

The technique used during this research is the vapour diffusion method, which is the most popular, as it can be used to screen a broad range of crystallisation conditions, using small amounts of materials, but can also be scaled up in order to obtain large crystals for X-ray diffraction analysis. Vapour diffusion can be separated into three procedures; the sitting drop, the hanging drop and the sandwich drop vapour diffusion techniques (Figure 1.3). A drop of 1:1 protein:precipitant solutions is usually used

and it is either supported by a surface (sitting drop), or is suspended from a surface (hanging drop). Furthermore, the drop can be in contact with both an upper and a lower surface (sandwich drop).

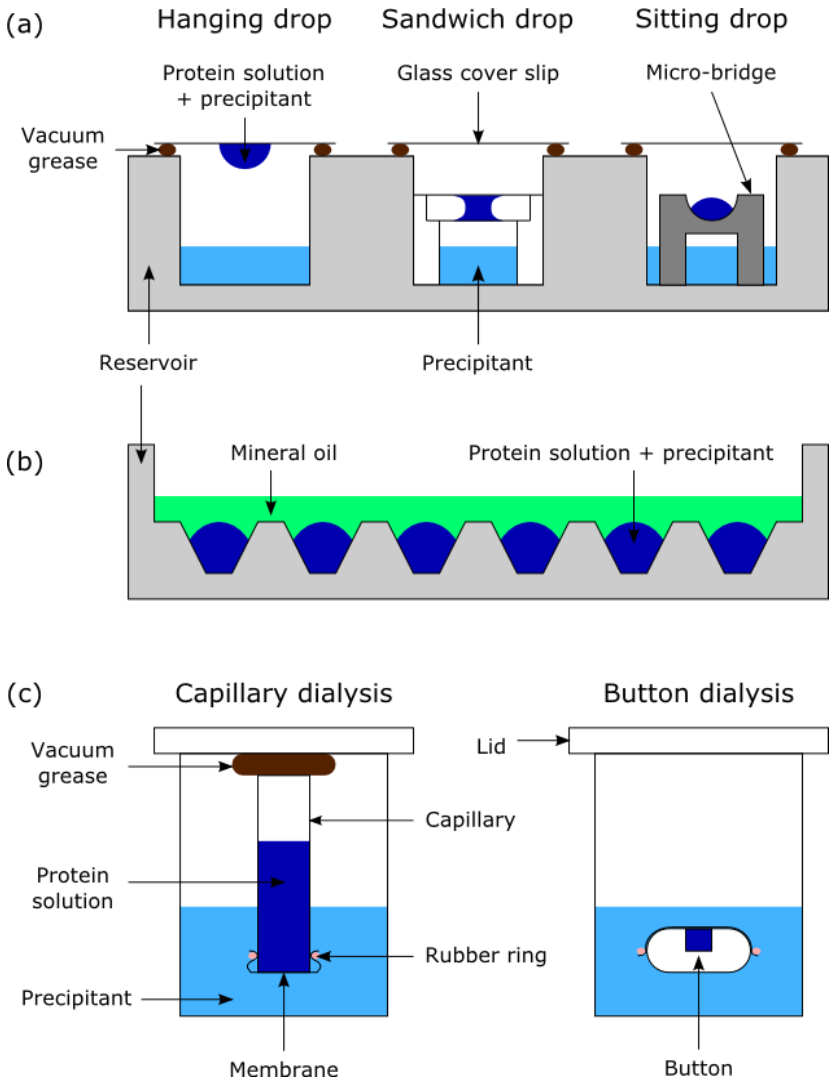

Figure 1.3. Schematic depicting three of the most common crystallisation techniques: (a) vapour-diffusion, (b) microbatch and (c) dialysis (17).

The entire system is sealed using vacuum grease and a cover slip, or using transparent crystallisation sealing tape (with a chemically inert adhesive). This prevents solvent being lost to the external environment. The difference in precipitant concentration between the drop and the reservoir solution causes water to diffuse away from the drop. This continues until

the concentration of the precipitant in the drop is the same as that of the reservoir well solution (Figure 1.4). Thus equilibration takes place through the vapour phase.

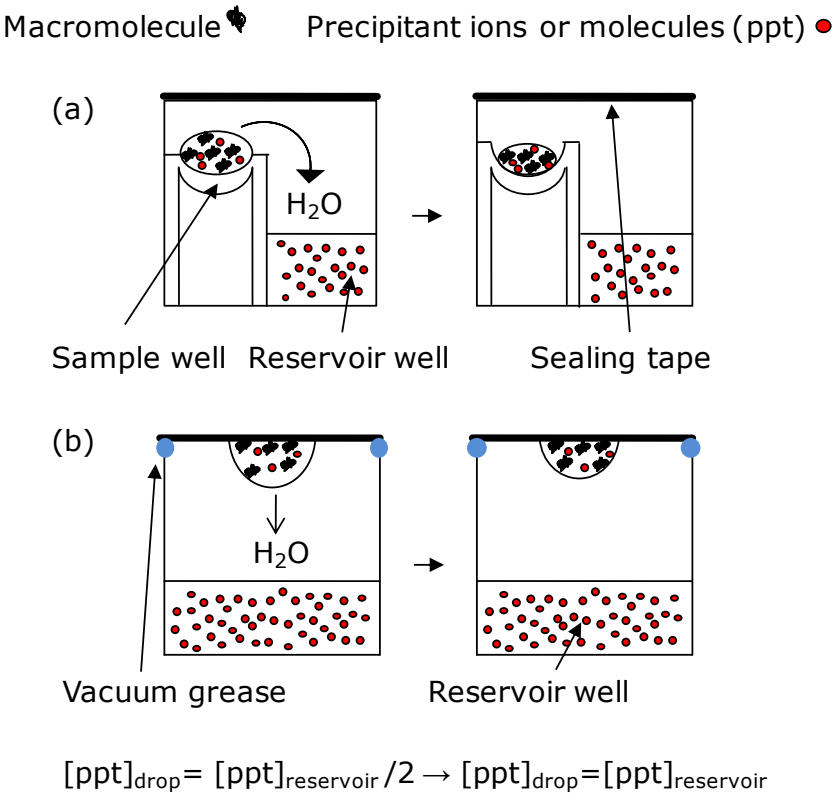

Figure 1.4. Schematic depicting (a) sitting and (b) hanging drop vapour diffusion crystallisation taking place in a single well environment. The reservoir has usually twice the concentration of precipitant than the sitting/hanging drop. Water loss from the drop via vapour diffusion, reduces the volume of the drop and as equilibration takes place, the concentration of the drop's components increase significantly.

Water loss from the drop to the reservoir solution causes reduction in the volume of the drop, which in turn increases the concentrations of all the solutes within it. Thus, precipitant and protein concentrations increase. Absorption of water by the air sealed in each microenvironment, at the beginning of the experiment, further increases the supersaturation level within the drop so that ideal nucleation levels of supersaturation are achieved (Figure 1.2).

The equilibration process can be slowed by reducing the surface area over which diffusion occurs, such as when the sandwich drop vapour diffusion technique is used, or by increasing the distance between the drop and the reservoir. For the hanging drop technique glass cover slips are used to suspend the drop. The cover slips are usually siliconised to obtain a hydrophobic surface, thus to prevent wetting and the drop from spreading (24). The same vapour diffusion principle applies to both sandwich and hanging drop techniques.

1.4.2. Batch Crystallisation

Batch crystallisation is the oldest and simplest crystallisation technique. In the batch method the concentrated protein solution is mixed with concentrated precipitant in a well, and the contents are covered with paraffin oil to prevent evaporation (Figure 1.3). This produces a final supersaturated solution immediately upon mixing which may lead to crystallisation (Figure 1.2). The volume of the drop and the precipitant concentration remain the same. Formation of protein crystals or protein precipitant can alter the protein concentration. Rapid equilibration during this technique can affect the rate of crystal growth and the quality of the crystals obtained.

Large amounts of solution that typically range from 50 µl to several millilitres are used in batch crystallisation, which can lead to larger crystals forming. In contrast, microbatch techniques require the use of smaller volumes (nanolitre to microlitre volumes) and are preferred for screening trials (17). Microbatch under oil, which was developed in the 1990s, is compatible with most precipitants, buffers and additives. However, this technique should not be used when small volatile organic molecules such

as dioxane, phenol and thymol are present, due to the fact that these chemicals are soluble in oil (27).

1.4.3. Dialysis Crystallisation

In the dialysis method the macromolecule solution is separated from the precipitant/crystallisation mixture by a membrane with a molecular weight limited permeability. The small precipitant molecules (ions, additives, buffers, etc.) can freely diffuse through the semi-permeable membrane in order for equilibration to take place, while the target macromolecules/proteins are unable to diffuse through the membrane (Figure 1.3) (18). In this technique the protein concentration is held constant while the precipitant concentration increases (Figure 1.2). Dialysis is used as a crystallisation method mainly for optimisation, once the conditions for crystallisation have been primarily identified by a more efficient method, such as vapour diffusion or microbatch crystallisation (27).

1.5. Nucleation

During the nucleation stage the formation of the first ordered aggregates signals the start of crystallisation, which is then followed by crystal growth. As mentioned in section 1.3, it is necessary to overcome the energy barrier that the crystalline state presents in comparison to the free solute molecules, thus it requires a higher supersaturation state than the one needed for crystal growth (24). Nucleation, and its mechanism, has been studied in detail as it is a key step towards crystal formation (28-30). Once critical nuclei have been formed and nucleation has been successful, crystal growth follows spontaneously (14, 24, 31). However, if nucleation

conditions persist, i.e. high supersaturation levels, then either multiple nuclei can result in amorphous precipitate or crystals that are too small in size to be used for analysis, such as X-ray crystallography, may form as a result (32). Nucleation can be affected by a number of factors, aside from supersaturation, such as well shape, drop volume and the geometry of the reservoir in a crystallisation experiment (24), given that changing the surface and volume energies, according to the Gibbs-Thomson equation also increases the nucleation frequency (29).

1.5.1. Homogeneous Nucleation

The crystallisation of a target macromolecule into a large, high quality, single crystal can be seen as the 'rate limiting step' in the structure elucidation process. Homogeneous nucleation occurs when nuclei spontaneously grow and form crystals in the bulk of the solution. Homonucleation crystallisation is less frequently employed in research due to the critical energy barrier that must be overcome for ordered nuclei to form.

1.5.2. Heterogeneous Nucleation

Heterogeneous nucleation takes place when the surface of a foreign substance lowers the energy barrier for the aggregation of molecules to occur, inducing nucleation, by acting as an 'anchor' for the crystallising molecules (Figure 1.5). Heterogeneous nucleation is perceived as a key step towards predicting, screening and directing protein crystallisation, given that it facilitates crystal formation at lower supersaturation values and increases nucleation frequency (33).

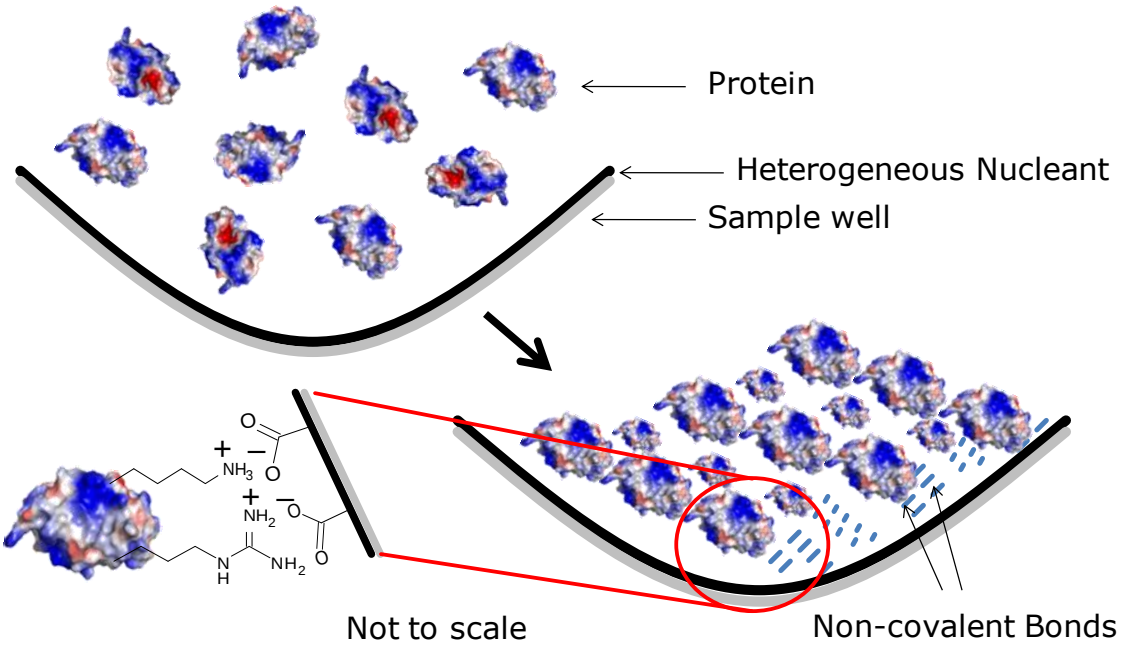

Figure 1.5. Schematic representation of heterogeneous nucleation during protein crystallisation. Nucleation occurs at surfaces preferentially. In general, biological macromolecules tend to adsorb to surfaces that offer attractive chemical, electrostatic or structural features that favour interaction, i.e. when there is functionality complementary between the heterogeneous nucleant surface and the crystallising molecules.

Examples of heterogeneous nucleation are seen when crystals grow attached to glass or plastic surfaces, or found associated with some type of debris, such as hair or fibres (34-36) (Figure 1.6). Time lapse video microscopy has been used to study the importance of surfaces in the earliest stages of crystal formation (37).

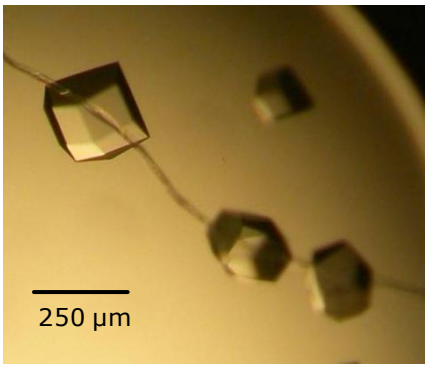

Figure 1.6. Photomicrograph showing hen egg-white lysozyme (HEWL) crystals nucleating on a fibre.

Nucleation occurs at surfaces preferentially. In general, biological macromolecules tend to adsorb to surfaces that offer attractive chemical, electrostatic or structural features that favour interaction, i.e. when there

is complementarity between the heterogeneous nucleant surface and the crystallising molecules (14). Molecules adsorbed to surfaces are spatially constrained, so they translate (move) in to two-dimensions rather than three, or are partially immobilised. This assists in nuclei formation, since the crystallising molecules are immobilised and can become part of an ordered array (14).

As such, a heterogeneous nucleant (also called substrate or heteronucleant) can be seen as a crystallisation catalyst; which helps lower the energy barrier for aggregation of molecules and induce nucleation, by concentrating or immobilising the crystallising molecules in such a way that they tend to nucleate and crystallise (14).

Homogeneous and heterogeneous nucleations proceed by chance attachment and dissociation of particles. However, in heterogeneous nucleation the induction period of forming critical nuclei is reduced (38), the supersaturation levels for crystallisation can be lowered (39, 40), while the observed nucleation density rates tend to increase (40), when compared to homogeneous nucleation.

Heterogeneous nucleation can occur when materials of various natures are introduced in crystallisation experiments either as surfaces of support to the drop containing the crystallisation target (macro)molecules or added directly into the crystallising mixture (23, 33, 40-43).

Heterogeneous nucleation, where the surfaces were made out of cross-linked polymers, has been used to selectively crystallise certain crystal forms of organic molecules (44-48), inorganic complexes (49) and extended networks (50). Heterogeneous nucleation of proteins has also been studied, using the following heterogeneous nucleants: minerals (51, 52), human hair (53), horse hair (54), polymers (23, 39, 40, 55, 56),

hydrophobic self-assembled monolayers (5), porous glass and silicon (43, 57, 58), silicon-based devices (59), and chemically treated glass surfaces (60, 61).

In parallel, research lead by E. Drioli over the last decade (62) has resulted in the development of a membrane-based technology, named "membrane crystallisation". Porous hydrophobic polypropylene membranes (Accurel® PP V8/2 HF) (63) were successfully utilised in crystallisation experiments to adjust the solution composition, from an undersaturated state to a supersaturated state and act as heterogeneous nucleants (64). These membranes used in vapour diffusion experiments (64, 65) have resulted in the crystallisation of inorganic (66), organic (67), (bio)macromolecular (68, 69) compounds, as well as active pharmaceutical ingredients, such as carbamazepine (anticonvulsant) (70).

1.6. Polymer Mediated Crystallisation

As mentioned above, various materials have been utilised as heteronucleants in recent research; however, they have not been proven as successful 'universal' heteronucleants that can be potentially employed in the crystallisation of most biological molecules. An ideal heteronucleant(s) would be able to promote crystallisation in most biological systems. The heteronucleant(s) should be able to be incorporated in the existing crystallisation formats available and have a diverse functionality, which is vital considering the unique three-dimensional structure and nature of biological macromolecules, as demonstrated by proteins.

A considerably successful candidate to the quest of a universal heteronucleant for small molecule single-crystal production has been

observed in the use of polymer-induced heteronucleation (71). This is due to the functional diversity observed in polymer libraries, which have been able to crystallise a broad range of pharmaceuticals (45, 72, 73) and other compound classes (50) from various aqueous and organic solutions.

Therefore, the range of polymer libraries available could also be used for heterogeneous nucleation in protein crystallisation. For example, Liberski et al. (47) used commercially available polymers as well as cross-linked and linear copolymers to create polymer microarrays (74), in order to screen well studied small molecules, such as carbamazepine and sulfamethoxazole, for polymorphism. This high throughput technique produced a large amount of data (3 molecules, each crystallised on 128 different polymers), and the crystals were characterised using optical and Raman spectroscopy. Unfortunately, the absence of polymer surface characterisation resulted in a lack of concluding remarks between crystal polymorphs and the surfaces which induced them.

Foroughi et al. (75) further demonstrated that polymer-induced heteronucleation can be applied to protein crystallisation successfully, by optimising the heteronucleant composition and crystallisation formats in order to crystallise a wide range of protein targets, also resulting in increased crystal size as well as the discovery of two new forms of concanavalin A and the structural elucidation of one of these forms.

Using parallel and combinatorial synthesis and varying monomers, catalysts, initiators and end-cappers can result in a vast array of polymers with different chemical characteristic being synthesised (76). There is great potential in heterogeneous nucleation and crystallisation of proteins in the presence of polymeric surfaces given that systems have now become automated and high throughput characterisation techniques are

being developed, in comparison to the first manual combinatorial polymer synthesis over a decade ago (77, 78). These scientific advances point to a potential future where polymeric film libraries can be employed as another factor when screening for the appropriate crystallisation conditions of a protein, or for crystallising different protein forms.

Further advantages in the use of polymer-induced heteronucleation were observed when research was conducted on the crystallisation of the proteins concanavalin A and hen egg-white lysozyme (HEWL), in the presence of polymeric films containing ionisable groups, cross-linked gelatine films with adsorbed poly-L-lysine or entrapped poly-L-aspartate, and silk fibroin with entrapped poly-L-lysine or poly-L-aspartate. Results showed that the presence of ionisable groups on the film surface affected protein crystallisation. From siliconised surfaces to uncharged polymeric surfaces to charged polymeric surfaces, there was a decrease in the induction time and protein concentration necessary for crystal nucleation to occur; while an increase in nucleation density was observed (40).

Another form of polymer-induced heterogeneous nucleation is the use of imprinted polymeric surfaces for the selective nucleation of crystals. Molecular imprinting is defined as "the construction of ligand selective recognition sites in synthetic polymers where a template (atom, ion, molecule, complex or a molecular, ionic or macromolecular assembly, including micro-organisms) is employed in order to facilitate recognition site formation during the covalent assembly of the bulk phase by a polymerisation or polycondensation process, with subsequent removal of some or all of the template being necessary for recognition to occur in the spaces vacated by the templating species" (79).

Initially, imprinted surfaces were used for the crystallisation of inorganic molecules. Copolymers, which were first imprinted with either calcium oxalate monohydrate or calcium oxalate dihydrate template crystals, were used to crystallise calcium oxalate from pure aqueous solutions and urine (80), demonstrating the use of imprinted surfaces for extraction/purification purposes. Other work showed that polymeric surfaces, imprinted with calcite, successfully directed the crystallisation of calcium carbonate into calcite crystals, while the crystallising conditions would normally yield aragonite crystals, a polymorph of calcium carbonate (81) (Figure 1.7).

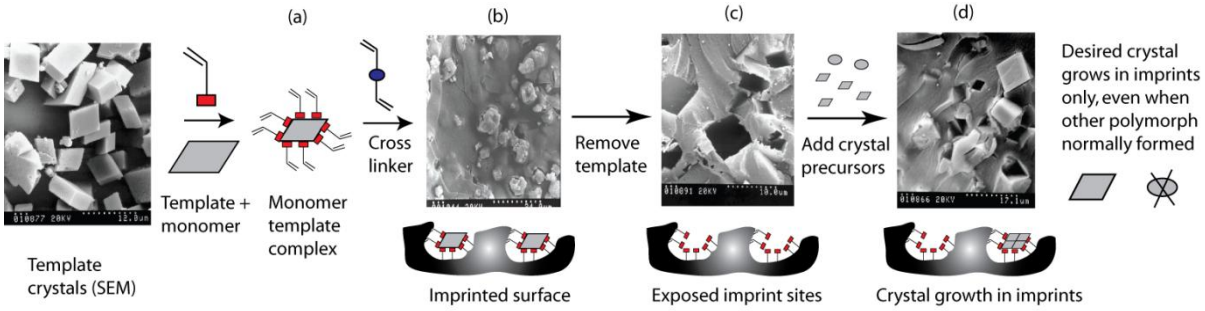

Figure 1.7. Selective crystallisation of calcium carbonate, in the form of calcite crystals, using molecularly imprinted surfaces. (a) The template rhombohedral calcite crystals form non-covalent bonds with the monomers, followed by cross-linking of monomers leading to the formation (b) of an imprinted surface. (c) Removal of calcium carbonate by mild acid wash exposes the imprinted sites. (d) Incubation of polymer surfaces with calcium and carbonate ions nucleates calcite only in the imprint sites under conditions which favour the formation of another polymorph of calcium carbonate, that of aragonite (81).

Recently, the principle of polymer-based imprinted surfaces employed in the crystallisation of inorganic molecules, has evolved into the creation and utilisation of protein-imprinted polymers, as heteronucleants, to direct protein crystallisation and avoid protein precipitant formation. Matsunaga et al. (82) successfully created protein-imprinted polymer films. Acrylic acid was utilised as the functional monomer in the creation of the imprinted polymer, while lysozyme was used as the template protein. After the removal of the template protein crystals, more lysozyme was successfully crystallised upon the polymer imprinted surface. The

effectiveness of protein-imprinted polymers was further tested by the previously mentioned group, by successfully crystallising five out of the six proteins tested (83). Moreover, Saridakis et al. (56) demonstrated the potential of molecularly imprinted polymer mediated protein crystallisation by crystallising proteins in the presence of polymer imprints under conditions which would normally yield no protein crystals. The formation of large single protein crystals and faster overall crystal formation were observed in the presence of protein imprinted polymers.

While all of the above mentioned work shows the clear potential in polymer mediated crystallisation, it is obvious that there is a great need for a clearer understanding of the mechanisms employed in polymer mediated heterogeneous protein crystallisation, which can be achieved via detailed surface analysis of the polymers and further experimental work with a broader range of challenging proteins, such as membrane proteins and other proteins which have yet to be successfully crystallised and characterised.

1.7. Proteins Utilised in the Thesis

Mutant human thioredoxin and wild type hen egg-white lysozyme (HEWL) were the two proteins used, for crystallisation, during this research. Thioredoxins are small (12 kDa) ubiquitous enzymes found in a variety of organisms, from archaea to humans. Lack of cytosolic thioredoxin is lethal to mammals. Thioredoxins are disulphide reductase enzymes that have a dithiol/disulphide active site. All thioredoxins have the same overall three-dimensional structure, known as the thioredoxin fold. This consists of five β-sheets surrounded by four α-helices and the conserved active site sequence is Trp-Cys-Gly-Pro-Cys (84, 85).

Thioredoxins, via thiol redox control, facilitate the redox regulation of protein function and signalling. In other words, thioredoxins maintain cytosolic proteins in their reduced state, while transcription factors, such as NF-kB, require thioredoxin reduction in order to bind to DNA (86). In turn, thioredoxin is reduced by electrons from NADPH via thioredoxin reductase (87). To date, structures of thioredoxins, wild type and mutant, from various organisms, have been obtained in solution by NMR (88, 89), as well as by X-ray diffraction of thioredoxin crystals (90, 91) (Figure 1.8).

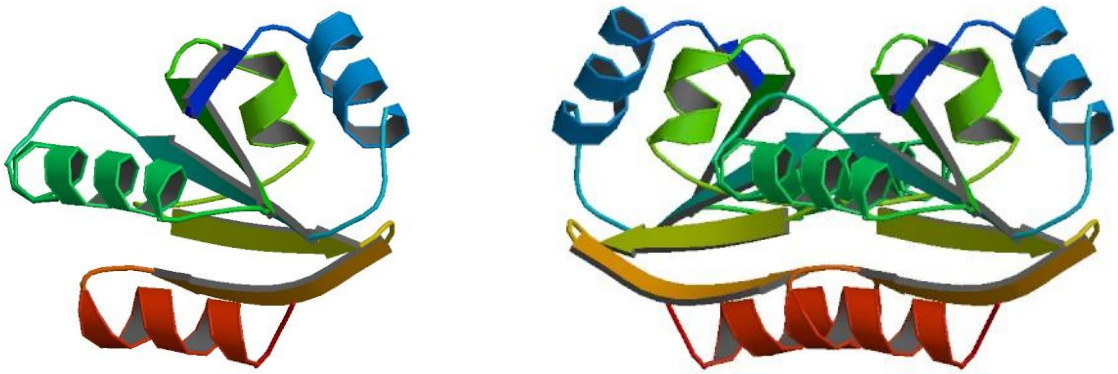

(a) (b)

Figure 1.8. Human thioredoxin structures, at 0.70 Å resolution, obtained by crystal X-ray diffraction data. The (a) asymmetric unit (smallest portion of the crystal structure to which symmetry operations can be applied in order to create a complete unit cell, i.e. the crystal repeating unit) of thioredoxin consists of five β-sheets and four α-helices with an active site of cysteines 32 and 35 in their oxidised form. The (b) assumed biological macromolecule, which is the assumed functional form of the protein, is a homodimer (two copies of the same asymmetric unit), which blocks the active site (85).

Lysozyme is a 129 amino acid long, single chain, enzyme protein. It is present in tears, saliva, mucus and in the egg-white of chickens. Lysozyme is a hydrolase and acts as a natural antibiotic by catalysing the hydrolytic cleavage of polysaccharides in the cell walls of bacteria, leading to bacterial lysis. Specifically, lysozyme hydrolyses the glycosidic bond between N-acetylmuramic acid and N-acetyl-D-glucosamine, and lyses gram positive bacteria, which have a peptidoglycan layer as their outer cell wall. Lysozyme has a molecular weight (Mw) of 14.3 kDa, four disulphide

bridges and is positively charged with a negatively charged active site crevice, formed by α-helices, where the polysaccharide substrate binds to be hydrolysed.

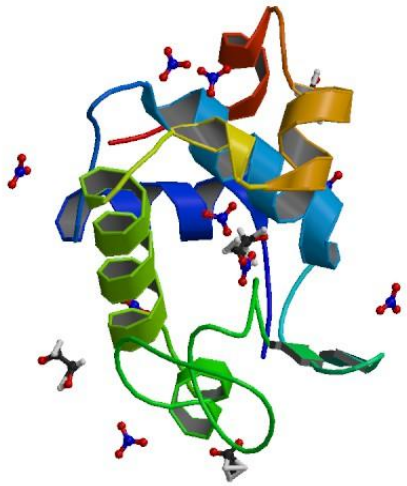

Figure 1.9. Hen egg-white lysozyme (HEWL) biological molecule structure, at 0.65 Å resolution, obtained by crystal X-ray diffraction. Lysozyme is a hydrolase that is formed by α–helices where polysaccharide substrates bind to be hydrolysed. The HEWL structure shown above was crystallised along with ligand molecules (acetate ions, 1,2-ethanediol and nitrate ions), which can be seen surrounding the single chain protein (92).

Lysozyme was utilised in this research as it is the most studied crystallisation system. This is due to the fact that HEWL is easily purified as well as being commercially available. Moreover, lysozyme crystallises with little effort and usually affords crystals within hours to a few days. HEWL has five structurally characterised crystal forms: monoclinic, triclinic, hexagonal, orthorhombic and tetragonal, as well as a less characterised form, that of needles (23). Finally lysozyme crystals afford high resolution X-ray diffraction patterns, with the highest resolution structure of 0.65 Å being published in 2007 (Figure 1.9) (92). Thus far, polymers have been used as heterogeneous nucleants as well as precipitants during HEWL crystallisation (23, 56, 93).

1.8. Aims and Objectives

In summary, predicting and controlling nucleation rates, or the occurrence of crystallisation, remains an elusive goal. The aim of this project is the utilisation of polymers in order to predict, screen and direct protein crystallisation. Polymers can be used as heterogeneous nucleants, in the form of films (adsorbed or plasma polymerised) or in solution. The polymeric surfaces require having a complementary surface chemistry to that of the target protein, in order to act as successful heteronucleants during the crystallisation of the target protein (Figure 1.5). Moreover, polymers can be utilised in order to aid in predicting, screening and directing protein crystallisation. The objective thus far has been to research the effect of polymer surfaces and polymers in solution to promote heterogeneous nucleation of known protein crystallisation systems.

Mutant human thioredoxin and hen egg-white lysozyme (HEWL) were used as model protein crystallisation systems in this research. Polyacrylic acid (PAA), polyvinyl alcohol (PVOH) and polyallylamine (PAAm) were used in protein crystallisation experiments due to their different functional groups. The above mentioned polymers were used, as physically adsorbed polymeric films and as precipitants in solution, during protein crystallisation. Surfaces were polymerised with acrylic acid (ppAA), allyl alcohol (ppAOH) and allylamine (ppAAm) in order to form substrates with similar functional groups to PAA, PVOH and PAAm respectively.

CHAPTER 2

2. Experimental and Characterisation Techniques

2.1. Introduction

The purpose of this chapter is to briefly introduce the theory behind the experimental and characterisation techniques that were employed in this research. Surface characterisation techniques, such as Water Contact Angle (WCA), Atomic Force Microscopy (AFM) and X-ray Photoelectron Spectroscopy (XPS) were utilised for the analysis of the substrates produced. Optical microscopy and X-ray crystallography were employed for protein crystal characterisation.

2.2. Experimental Techniques

2.2.1. Piranha Etching

Piranha etching, (also known as: Piranha solution or Caro's acid or permonosulphuric acid or peroxymonosulphuric acid), was first prepared by Heinrich Caro in 1898. It is a mixture of sulphuric acid and hydrogen peroxide, of a 3:1 ratio, which can be utilised to clean substrate surfaces from organic residues. The Piranha acid is a powerful oxidant and can react explosively with certain organic compounds. Once hydrogen peroxide is added in sulphuric acid a self-starting, exothermic reaction takes place. A second type of Piranha solution exists, which utilises ammonium hydroxide with hydrogen peroxide (3:1 ratio), however this is not a self-starting reaction and requires heating to 60°C for the reaction to occur. This base Piranha solution is utilised when the substrates treated have a low tolerance to acids.

Piranha etching removes organic contaminants and oxidises the heavy metal salts present as contaminants on the surface of glass substrates, resulting in a chemically clean and topographically 'smooth' surface, which can be assessed using Atomic Force Microscopy (AFM) (section 2.3.2). The surface chemistry change of Piranha etched glass can be assessed by taking Water Contact Angle (WCA) (section 2.3.1) measurements and conducting X-ray Photoelectron Spectroscopy (XPS) (section 2.3.3) on the substrates.

When planning to utilise plasma polymerised glass substrates in protein crystallisation experiments it is prudent to ensure that the glass surfaces are efficiently cleaned so that contaminants do not affect the crystallisation results. The topographical change following treatment with Piranha solution also ensures that a smooth and even plasma polymer deposition can take place.

2.2.2. Plasma Polymerisation

Figure 2.1 provides a schematic illustration of a plasma deposition chamber. In the chamber during operation, a monomer is subjected to an electromagnetic field under low pressure. The electrical discharge causes electrons to flow and interact with the monomer leading to the activation of the monomer. The ionised gas created, which is also known as plasma, reacts with the substrate forming a highly cross-linked, polymer-like material, known as the plasma polymer, on the substrate surface. The structural difference between conventional polymers and plasma polymers can be seen in Figure 2.2.

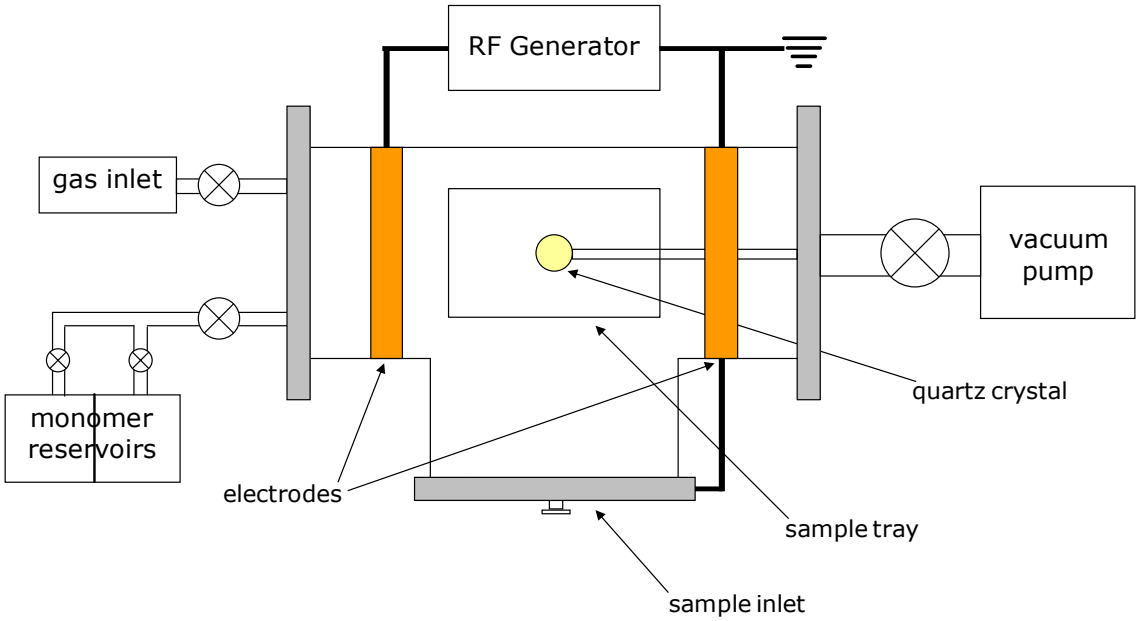

Figure 2.1. Schematic of a plasma deposition chamber. During operation, a monomer is subjected to an electromagnetic field under low pressure within the main chamber. The electrical discharge causes electrons to flow and interact with the monomer leading to the activation of the monomer. The ionised gas created (plasma), reacts with the substrate forming a highly cross-linked, polymer-like material, known as the plasma polymer, on the substrate surface.

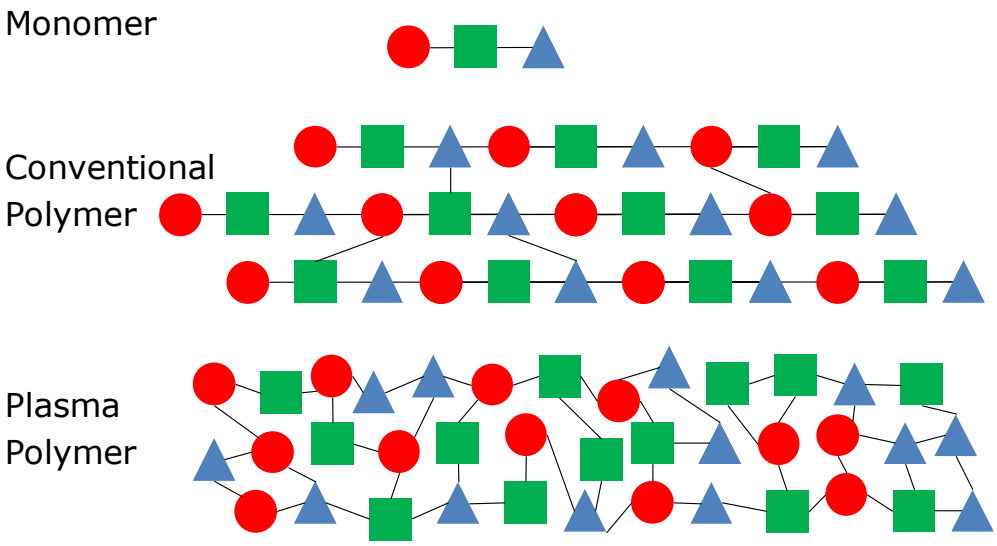

Figure 2.2. Schematic demonstrating the structural difference between conventional and plasma polymers.

Plasma polymers are employed in a range of applications due to the fact that they provide great coating adhesion on most substrates and exhibit chemical, mechanical as well as thermal stability. In this research they were utilised since they provide a uniform chemistry across the treated

surface, with different functional groups depending on the monomer used; and should provide a stable enough coating for protein crystallisation to occur. Figure 2.3 shows the three plasma polymerised substrate types used in this research. At this point it should be noted that prior to plasma polymer deposition, substrates were usually treated with an inert gas, in this case oxygen, which is also ionised in order to create an etching plasma in order to further clean and prepare the substrates' surfaces.

Surfaces were polymerised with acrylic acid (ppAA), allyl alcohol (ppAOH) and allylamine (ppAAm) in order to form substrates with similar functional groups to PAA, PVOH and PAAm respectively, which were used in protein crystallisation as physically adsorbed polymers and as polymers in solution.

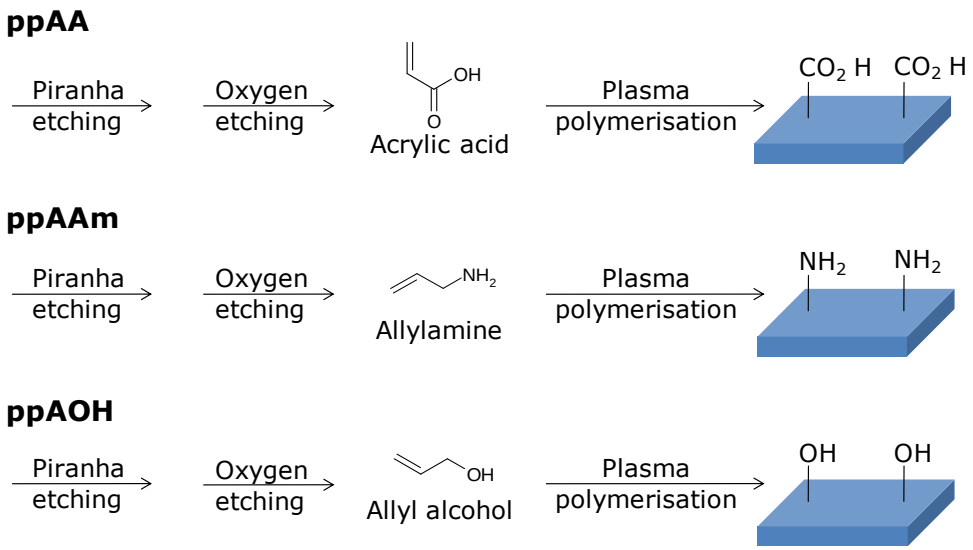

Figure 2.3. Schematic showing the preparation of the three types of plasma polymerised surfaces: (ppAA) plasma polymerised acrylic acid, (ppAAm) plasma polymerised allylamine and (ppAOH) plasma polymerised allyl alcohol.

2.3. Surface Characterisation Techniques

2.3.1. Water Contact Angle

The contact angle (θ) is a quantitative measure of the wetting of a solid by a liquid, usually water, and it is a technique that is broadly accepted for

material surface analysis related to adhesion and absorption. It is defined geometrically as the angle formed by a liquid at the three phase boundary where a liquid, gas and solid intersect.

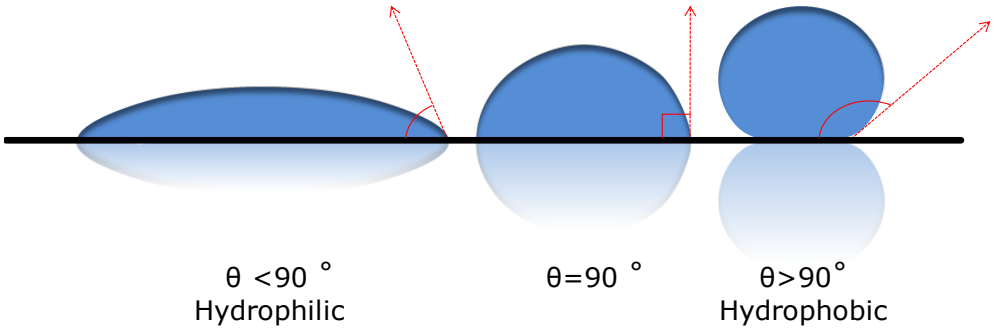

Figure 2.4. Schematic demonstrating how the internal angle (θ) of a water droplet can change depending on the interaction between water molecules and a solid surface. Hydrophilic surfaces attract the water molecules resulting in decreased internal angles (θ<90°), while hydrophobic surfaces result in weaker attractions with the water molecules and higher internal angles (θ>90°).

In this research, water contact angles (WCA) were measured at room temperature using a contact angle goniometer. WCAs were recorded so as to determine the substrate surfaces in terms of their hydrophobicity/hydrophilicity, following chemical treatment such as Piranha etching, which affects the nature of the substrate surface chemistry. Figure 2.4 demonstrates the droplet spreading that occurs when water comes in contact with a hydrophilic surface, resulting in θ<90°being observed, while hydrophobic surfaces tend to have a θ>90° when measured.

2.3.2. Atomic Force Microscopy

Atomic Force Microscopy (AFM) is a high resolution scanning probe microscopy. In contrast to traditional microscopy, in AFM there is a direct mechanical contact between the probe and the surface that is being sampled/scanned at the time, as it can be seen in Figure 2.5.

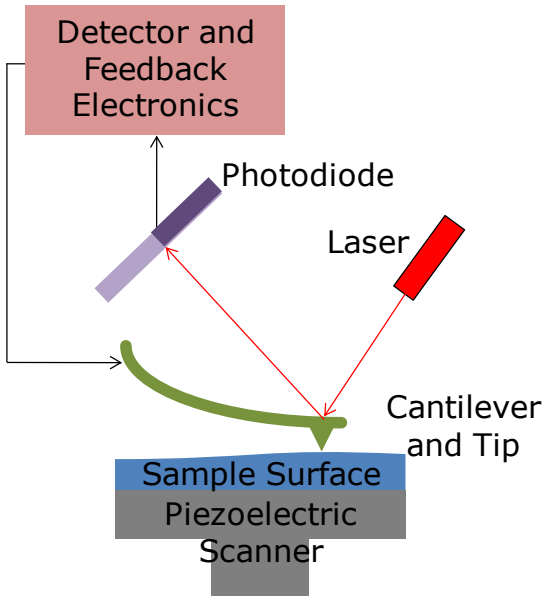

Figure 2.5. Schematic of the components in an Atomic Force Microscope (AFM). AFM utilises a sharp probe, which is a tip on the end of a cantilever, moving over the surface of a sample in a raster scan. The cantilever bends in response to the force between the tip and the sample. The movements of the cantilever tip are detected by a beam deflection system, where a laser beam gets deflected upon the cantilever's end and is detected by a photodiode.

Like all other scanning probe microscopes, the AFM utilises a sharp probe moving over the surface of a sample in a raster scan. In the case of the AFM, the probe is a tip on the end of a cantilever which bends in response to the force between the tip and the sample. The movements of the cantilever tip are detected by a beam deflection system, where a laser beam gets deflected upon the cantilever's end and is detected by a photodiode. AFM can be used for topographic measurements, measurements of attractive and repulsive forces between the probe tip and the sample surface, and measurements of the mechanical properties of the sample. AFM can image almost any type of surface including polymers, ceramics, glass and even biological samples.

In this thesis, AFM was used to image the topography of glass substrates at various stages of their treatment, from Piranha etching all the way to their plasma polymerised condition, prior to their use as heteronucleant surfaces in protein crystallisation.

2.3.3. X-ray Photoelectron Spectroscopy

X-ray Photoelectron Spectroscopy (XPS) is a quantitative surface chemistry technique that analyses the top 10 nm of a sample surface. Due to the fact that XPS is a highly sensitive surface technique, even the smallest amount of contamination, such as a single fingerprint, can alter/mask the surface chemical composition of a sample.

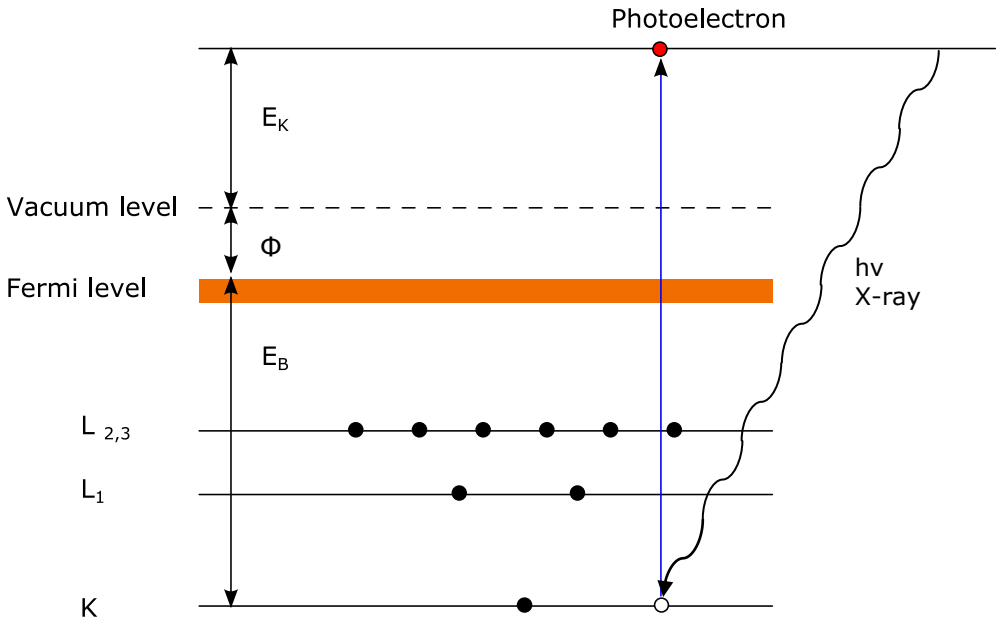

Figure 2.6. Schematic of the photoelectron emission in X-ray Photoelectron Spectroscopy (XPS) as a result of sample surface irradiation.

Under ultra-high vacuum the sample is irradiated using an X-ray source, in this case a mono-chromated Al kα source (1486.6 eV), causing photoelectrons to be emitted from the sample surface (Figure 2.6). An energy analyser determines the binding energy of each of the photoelectrons collected by an electron collection lens. The binding energy along with the intensity of the photoelectron peak detected is used to determine the identity, chemical state and quantity of the elements present upon the sample surface. Since the photoelectrons released, following irradiation of the sample, can result in a positive charge built-up along the sample surface, a charge neutraliser filament above the sample

gives a flux of low energy electrons providing uniform charge neutralisation.

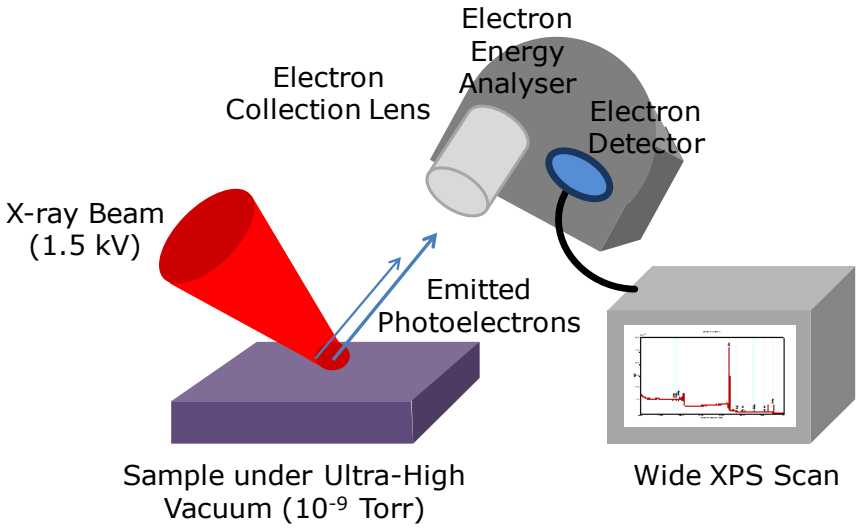

Figure 2.7. Schematic of the components of an X-ray Photoelectron Spectroscopy (XPS) system. Under ultra-high vacuum the sample is irradiated using an X-ray source causing photoelectrons to be emitted from the sample surface. An energy analyser determines the binding energy of each of the photoelectrons collected by an electron collection lens. The binding energy along with the intensity of the photoelectron peak detected is used to determine the identity, chemical state and quantity of the elements present upon the sample surface.

Figure 2.7 is a schematic of the main components of an XPS system, such as the one used in this research. As a surface chemistry analysis technique, XPS is ideal for contaminant detection, and was used to analyse glass substrates that were Piranha etched, oxygen etched and plasma polymerised with different monomers, prior to their use as heteronucleant surfaces in protein crystallisation.

2.4. Protein Crystal Characterisation Techniques

2.4.1. Optical Microscopy

An optical stereomicroscope, which uses visible light and a system of lenses, was employed to quantitatively observe the crystallisation trays used in this research.

Isotropic materials, such as glass and sodium chloride crystals, have an index of refraction that is equal throughout their structure, as their

mechanical properties have identical values in all directions. However, most physical properties of a wide variety of crystals, including liquid and macromolecular crystals, show variation throughout their structure. This anisotropy in the optical properties of crystals is known as birefringence. A birefringent material will cause a light ray to split into two beams as it passes through it. Protein crystals can be viewed under a light microscope with polarising optics in order for birefringence to be observed and to be able to differentiate between protein crystals (birefringent) and non-birefringent crystal salts/amorphous precipitate.

The attachment of a polarising filter to the optical stereomicroscope (cross polar microscopy) was used to confirm the presence of birefringent protein crystals (instead of salt crystal formation) as a primary qualitative technique. Lysozyme and thioredoxin crystals are both coloured when viewed via cross polar microscopy, while isotropic salt crystals appear clear. A digital camera attached to the microscope was used to image the crystals and obtain photomicrographs of the crystallisation wells.

2.4.2. X-ray Crystallography

X-ray crystallography is a common protein crystal characterisation technique, used to determine the arrangement of atoms within a crystal. A schematic overview of x-ray crystallography can be seen in Figure 2.8.

In x-ray crystallography, electrons, from an x-ray source, hit a copper target to produce a primary x-ray beam. The x-ray beam hits the sample crystal, which is mounted on a goniometer and is gradually rotated. The diffracted x-rays are detected electronically and by collecting these two-dimensional diffraction patterns, from various angles of the sample crystal, it is possible to convert the information into a three-dimensional map of

the electron density of the crystal. Using computational calculations it is then possible to extrapolate a probable three-dimensional structure for the target molecule crystallised. In this research, x-ray diffraction patterns were obtained from the protein crystals produced in order to confirm their identities, as their protein structure has already been researched and elucidated.

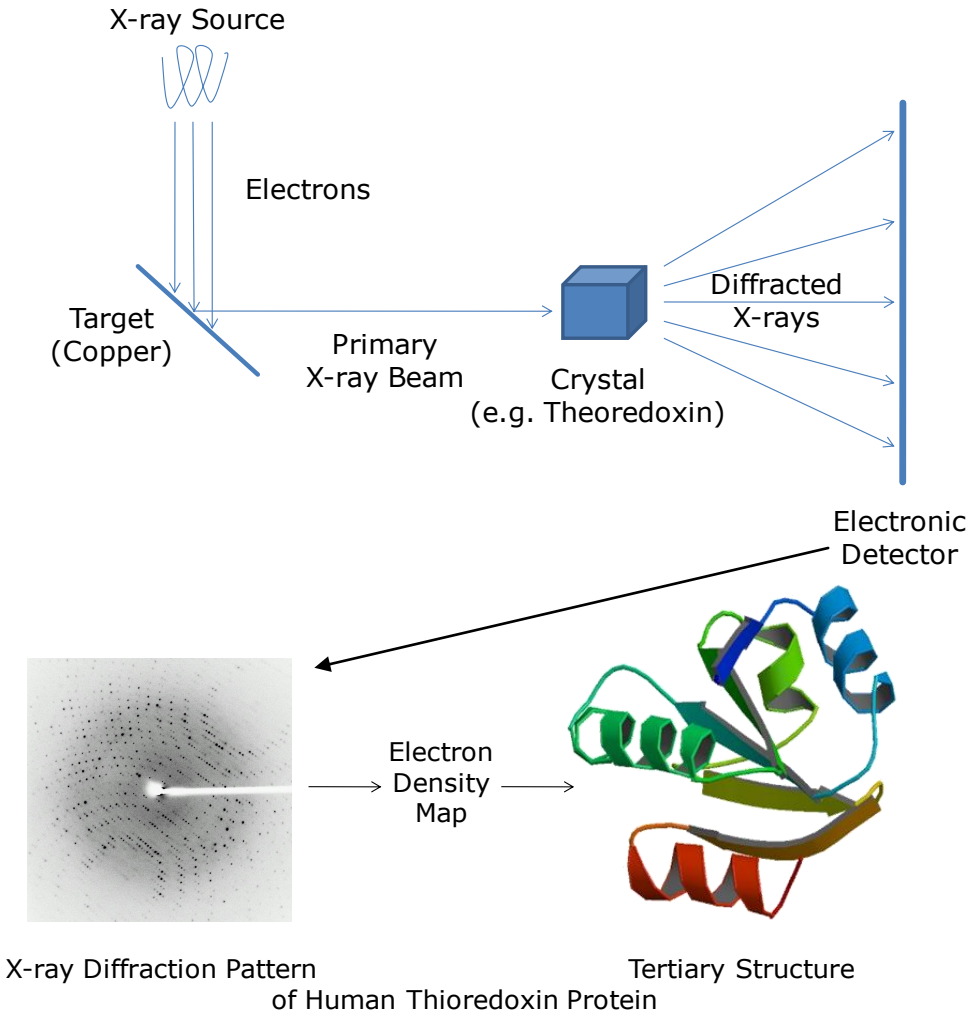

Figure 2.8. Schematic overview of X-ray crystallography. Electrons hitting a copper target create a primary x-ray beam which is diffracted by a crystal. The diffracted x-rays strike an electronic detector and create an x-ray diffraction pattern. Computational calculations are performed in order to create an electron density map. Finally, a three-dimensional structural rendering of the crystal is then predicted (tertiary structure of human thioredoxin shown above was obtained by Weichsel et al. (85)).

CHAPTER 3

3. Materials and Methods

3.1. Physically Adsorbed Polymers and Protein Crystallisation

3.1.1. Preparation of Polymer Blends

PAA ~50 kDa (25% in H_2O) was purchased from Polysciences, PVOH ~55 kDa was purchased from Aldrich and PVP ~72 kDa was purchased from MP Biomedicals (Figure 3.1). HPLC grade methanol (MeOH) was obtained from Fisher Scientific. Polymer solutions of PAA in water (H_2O), PVOH in H_2O and PVP in MeOH were prepared at a 1% w/v concentration. Using these polymer solutions, polymer blends of PAA with PVOH, PAA with PVP, and PVP with PVOH were prepared in v/v ratios of 0:10, 1:9, 2:8, 3:7, 4:6 5:5, 6:4, 7:3, 8:2, 9:1 and 10:0. Thus, twenty-seven polymer blends and three pure polymer solutions were prepared, each with a total volume of 100 µl. All the solutions were centrifuged at 13,000 rpm for 5 min at 4°C.

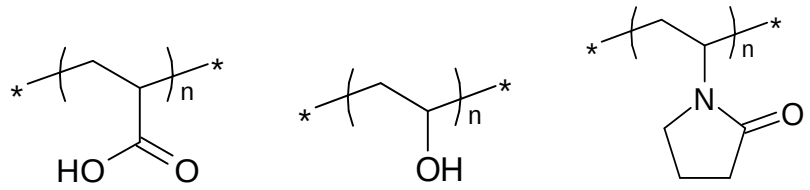

P AA PVOH PVP

Figure 3.1. Chemical structures of polyacrylic acid (PAA), polyvinyl alcohol (PVOH) and polyvinyl pyrrolidone (PVP).

3.1.2. Preparation of Crystallisation Plate – Method I

Art Robbins Intelli-Plate™ 96-2 well crystallisation plate is commercially available from Hampton Research (Figure 3.2). For each polymer solution (prepared in section 3.1.1) 8 µl aliquots were manually pipetted into the large sample wells of the crystallisation plate, in triplicate for reproducibility. Each corresponding small sample well contained no

polymer and was used as a control. Three large sample wells and their corresponding small wells were also kept polymer-free for control purposes. Two plates were prepared, one for each protein crystallisation protocol.

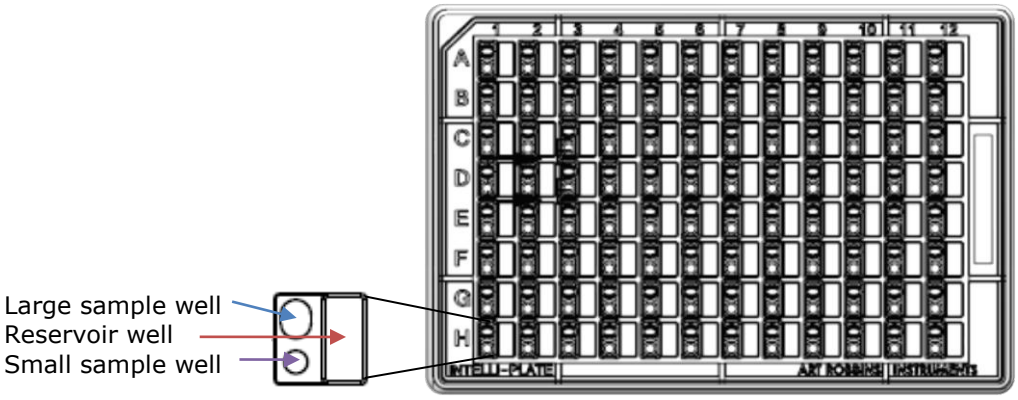

Figure 3.2. Rendering of the Art Robbins Intelli-Plate™ 96-2 well crystallisation plate. It is made out of polystyrene and has 96 reservoir wells (100 µl max fill volume) with two different size corresponding sample wells (10 µl and 4 µl max fill volume). Commercially available from Hampton Research.

The crystallisation plates were loosely covered with aluminium foil and the solvents of the polymer solution drops were left to evaporate completely at room temperature (RT) (~2 h).

3.1.3. Crystallisation Protocol for Human Thioredoxin Trigonal Crystals

Mutant human thioredoxin, (Cys^{35} and Cys^{73} mutated to Ser^{35} and Arg^{73} respectively, pI: 4.97), 60 mg/ml in a buffer of 20 mM TRIS-HCl, 150 mM NaCl, pH 7.4, was kindly provided by Dr Gareth Hall and was centrifuged at 13,000 rpm for 5 min at 4°C. 0.1 M sodium acetate, 30% v/v PEG 300, pH 4.6 buffer was prepared and filtered through a 0.2 µm cellulose acetate membrane filter.

Thioredoxin crystallisation was performed on a 96-2 well crystallisation plate (prepared in section 3.1.2) that contained polymer blend films, using the sitting drop vapour diffusion technique. Specifically, protein solution (1 µl) and buffer (1 µl) were aliquoted into each sample well (large and

small) and 48 µl of buffer were aliquoted in each reservoir well of the crystallisation plate. The final concentration of thioredoxin in each sample well was 30 mg/ml. All sample wells containing PAA turned opaque when protein and buffer solutions were aliquoted into them. The plate was then sealed and incubated at 19^{o}C. Crystals started forming after 13 days.

3.1.4. Crystallisation Protocol for Tetragonal HEWL Crystals – Method I

HEWL was purchased from Sigma (catalogue number: L6876, EC: 3.2.1.17, pI: 11.35, lysozyme activity: ~50,000 units/mg protein). 0.1 M sodium acetate solution at pH 4.8 was prepared and filtered through a 0.2 µm cellulose acetate membrane filter. This was used to prepare the 50 mg/ml HEWL solution, which was then centrifuged at 13,000 rpm for 5 min at 4^{o}C. 0.1 M sodium acetate, 8% w/v NaCl, pH 4.8 buffer was prepared and filtered through a 0.2 µm cellulose acetate membrane filter.

HEWL crystallisation was performed on a 96-2 well crystallisation plate (prepared in section 3.1.2) that contained polymer blend films, using the sitting drop vapour diffusion technique. Specifically, protein solution (2 µl) and buffer (2 µl) were aliquoted into each sample well (large and small) and 46 µl of buffer were aliquoted in each reservoir well of the crystallisation plate. The final concentration of HEWL in each sample well was 25 mg/ml. All sample wells containing PAA turned opaque when protein and buffer solutions were aliquoted into them. The plate was then sealed and incubated at 19^{o}C. Crystals formed within 24 h.

NB: When sealing the plate, the drops of protein and buffer contained within the small sample wells of the crystallisation plate, tended to touch the sealing tape. Thus, from then on the total volume aliquoted in all sample wells was not more than 2 µl.

3.1.5. Preparation of Polymer Solutions

PAA ~50 kDa (25% in H_2O) and PAA ~1,000 kDa were purchased from Polysciences. PAA ~100 kDa (35% in H_2O), PAA (~0.1% cross-linked) ~3,000 kDa and PAA (~0.1% cross-linked) ~4,000 kDa were purchased from Sigma.

The following polymer solutions were prepared: PAA (~50 kDa) in H_2O at concentrations of 0.01%, 0.1%, 1%, 1.5%, 2.0%, 2.5%, 3%, 3.5%, 4%, 4.5%, 5% (w/v); PAA ~100 kDa in H_2O at concentrations of 0.1% and 1% (w/v); PAA ~1,000 kDa in H_2O at concentration of 0.1% (w/v); PAA ~3,000 kDa in H_2O at concentration of 0.1% (w/v); and PAA ~4,000 kDa in H_2O at concentration of 0.1% (w/v). All polymer solutions were centrifuged at 13,000 rpm for 5 min at 4^{o}C.

3.1.6. Preparation of Crystallisation Plate – Method II

In order to avoid contamination, the Art Robbins Intelli-Plate^{TM} 96-2 well crystallisation plate (Figure 3.2) preparation was conducted in a laminar flow cabinet. For each polymer solution (prepared in section 3.1.5) 8 µl aliquots were manually pipetted into large sample wells of the crystallisation plate, in triplicate for reproducibility. The solvent was left to evaporate completely at RT for 2 h. Each corresponding small sample well contained no polymer and was used as a control. Thirty-six large sample wells and their corresponding small wells were also kept polymer-free for control purposes.

For the polymers solutions PAA ~100 kDa 0.1% in H_2O, PAA ~1,000 kDa 0.1% in H_2O, PAA ~3,000 kDa 0.1% in H_2O and PAA ~4,000 kDa. 0.1% in H_2O, an extra set of 8 µl aliquots were manually pipetted into the large sample wells of the crystallisation plate, in triplicate. The solvent was left

to evaporate completely at RT for 2 h. This was repeated twice more, so that (8 µg/8 µl x 3=) 24 µg of PAA were deposited in each of these wells. This was done due to the fact that small volumes of high molecular weight polymer solutions were highly viscous.

3.1.7. Crystallisation Protocol for Tetragonal HEWL Crystals – Method II

HEWL crystallisation was performed on a 96-2 well crystallisation plate (prepared in section 3.1.6) that contained PAA films, using the sitting drop vapour diffusion technique. The same protocol was used as described in section 3.1.4, but with different volumes of protein and buffer being aliquoted. The pipetting was conducted in a laminar flow hood to avoid contamination. Specifically, 1 µl of protein (50 mg/ml HEWL in 0.1 M sodium acetate solution at pH 4.8) and 1 µl of buffer (0.1 M sodium acetate, 8% w/v NaCl, pH 4.8) were aliquoted into each sample well (large and small) of the crystallisation plate. Also 48 µl of buffer were aliquoted in each reservoir well. Each sample well had a HEWL concentration of 25 mg/ml. All sample wells containing PAA turned opaque when protein and buffer solutions were aliquoted into them. The crystallisation plate was sealed and incubated at 19^{o}C. Crystals formed within 24 h.

3.1.8. Solubility Test

During the previous crystallisation experiments (sections 3.1.3, 3.1.4 and 3.1.7) sample wells that contained PAA turned opaque following the addition of protein/buffer solution. This could be due to PAA film delaminating or redissolving. PAA is water soluble and the buffer (0.1 M sodium acetate, 8% w/v NaCl, pH 4.8) and protein solution (50 mg/ml

HEWL in 0.1 M sodium acetate solution at pH 4.8) used in HEWL crystallisation are aqueous solutions.

Table 3.1 shows the concentration of the PAA aliquots pipetted into the crystallisation plate during the experiment described in section 3.1.6, prior to solvent evaporation, and the corresponding PAA concentration in each of the sample wells, provided that PAA redissolved completely in 2 µl of protein/buffer solution.

Concentration of PAA 8 µl aliquots prior to solvent evaporation	**Concentration of redissolved PAA film in 2 µl protein/buffer solution**
PAA 0.01%	(0.8 µg / 8 µl →0.8 µg / 2 µl =0.4 µg/µl) PAA 0.04%
PAA 0.1%	PAA 0.4%
PAA 0.3% (= 0.1% x 3)	PAA 1.2%
PAA 1%	PAA 4%
PAA 1.5%	PAA 6%
PAA 2%t	PAA 8%
PAA 2.5%	PAA 10%
PAA 3%	PAA 12%
PAA 3.5%	PAA 14%
PAA 4%	PAA 16%
PAA 4.5%	PAA 18%
PAA 5%	PAA 20%

Table 3.1. Concentration of the polyacrylic acid (PAA) aliquots pipetted into the crystallisation plate during the experiment described in section 3.1.6, prior to solvent evaporation, and the corresponding PAA concentration in each of the sample wells, provided that PAA redissolved completely in 2 µl of protein/buffer solution.

Freeze-dried PAA ~50 kDa (400 mg) and freeze-dried PAA ~100 kDa (80 mg) were weighed in two separate clear plastic 5 ml vials. Buffer (1 ml) and protein solution (1 ml) were added in each vial (400 mg/2 ml – PAA

20% and 80 mg/2 ml – PAA 4%). PAA ~1,000 kDa (48 mg), PAA (~0.1% cross-linked) ~3,000 kDa (48 mg) and PAA (~0.1% cross-linked) ~4,000 kDa (48 mg) were weighted in three separate clear plastic 5 ml vials. Buffer (2 ml) and protein solution (2 ml) were added in each vial (48 mg/4 ml – PAA 1.2%). All eight solutions turned cloudy during brief mixing. The PAA visually appeared to have dissolved in all solutions.

3.1.9. Crystal Imaging

Images of the crystals were obtained using a Leica MZ16 Stereomicroscope (63x magnification), with a Leica CLS1 50X fan-cooled light source, connected to a Nikon Coolpix 4500 digital camera (4.0 megapixels).

3.2. Polymers as Precipitants and Protein Crystallisation

3.2.1. Preparation of Stock Solutions

The solubility test (section 3.1.8) showed that PAA of various molecular weights dissolves when mixed in protein and buffer solution used in the crystallisation protocol of HEWL. Thus, it was necessary to observe whether PAA, of various molecular weights and concentrations, dissolved in the reservoir solution of the crystallisation protocol of HEWL would give similar results to experiment 3.1.7.

These commercially available polymers, PAA ~50 kDa (25% in H_2O), PAA ~100 kDa (35% in H_2O) and PAA ~1,000 kDa (see section 3.1.5 for materials), were used in order to prepare the following polymer solutions: PAA ~50 kDa 20% in H_2O pH 4.8, PAA ~100 kDa 20% in H_2O pH 4.8 and PAA ~1,000 kDa 1% in H_2O pH 4.8. The polymer solutions were then filtered using a 0.2 μm cellulose acetate membrane filter. Also a stock

buffer solution of 0.25 M Na Acetate 20% NaCl pH 4.8 was prepared and filtered using a 0.2 µm cellulose acetate membrane filter.

Using the above mentioned pH-altered polymer solutions and the stock buffer solution the following reservoir solutions were prepared at a final volume of 1 ml or 2 ml: PAA (~50 kDa) 0.02%, 0.08%, 0.2%, 0.8%, 2%, 3%, 4%, 5%, 6%, 7%, 8%, 9%, 10%, 11% and 12% in 0.1 M sodium acetate 8% NaCl pH 4.8; PAA (~100 kDa) 0.02%, 0.08%, 0.2%, 0.8%, 2%, 3%, 4%, 5%, 6%, 7%, 8%, 9%, 10%, 11% and 12% in 0.1 M sodium acetate 8% NaCl pH 4.8; and PAA (~1,000 kDa) 0.002%, 0.008%, 0.02%, 0.08% and 0.2% in 0.1 M sodium acetate 8% NaCl pH 4.8.

3.2.2. Crystallisation Protocol for Tetragonal HEWL Crystals– Method III

HEWL crystallisation was performed on Art Robbins Intelli-Plate^{TM} 96-2 well crystallisation plates (Figure 3.2), using the sitting drop vapour diffusion technique. The same protocol was used as described in section 3.1.4, but with different volumes of protein and buffer being aliquoted. All manual pipetting was conducted on an open lab bench. Specifically, 50 µl of each of the reservoir solutions prepared in section 3.2.1 was aliquoted in triplicate in the reservoir wells of the crystallisation plates. 1 µl of protein (50 mg/ml HEWL in 0.1 M sodium acetate solution at pH 4.8) and 1 µl reservoir solution taken from each reservoir were aliquoted into corresponding sample wells (big and small) of the crystallisation plate. In each sample well, the PAA concentration was half of the polymer concentration in the reservoir, while HEWL concentration was 25 mg/ml. For control, some wells contained no polymer in their reservoir solution and some wells contained no protein. All sample wells containing PAA turned opaque when protein and buffer solutions were aliquoted into

them. The crystallisation plate was sealed and incubated at 19°C. Crystals formed within 24 h.

3.2.3. Crystal Imaging

Images of the crystals were obtained as described in section 3.1.9.

3.3. Plasma Treated Surfaces and Protein Crystallisation

3.3.1. Preparation of Plasma Polymers

3.3.1.1. Piranha Etching

HPLC grade acetone and hydrogen peroxide (30% in H_2O) were purchased from Fluka (Sigma Aldrich). Sulphuric acid 95% laboratory reagent grade was purchased from Fisher Chemicals. Prior to Piranha etching, glass cover slips (Scientific Laboratory Supplies Ltd, No. 2 thickness, 22 x 22 mm) were washed using acetone and dried under a nitrogen stream. The glass substrates were then immersed in Piranha solution of 3:1 (v/v) sulphuric acid / hydrogen peroxide for 30 min (exothermic reaction). The substrates were then turned over and immersed in Piranha solution for another 30 min. The substrates were then rinsed extensively under running deionised water, followed by drying under a nitrogen stream.

3.3.1.2. Plasma Treatment

Acrylic acid, allylamine and allyl alcohol were obtained from Aldrich. They were used as received, save three freeze-thaw cycles to remove dissolved gases prior to use. The substrates for plasma polymerisation (Scientific Laboratory Supplies Ltd glass cover slips, No. 2 thickness) were acetone washed and Piranha etched prior to plasma treatment. The substrates

were placed in a plasma deposition reactor. All substrates were first oxygen plasma etched for 5 min at 20 W incident power, ~300 mTorr pressure. The plasma deposition parameters for plasma polymerised acrylic acid (ppAA) and allylamine (ppAAm) plasma were: 20 W power and 300 mTorr pressure for ~28 min. For the deposition of plasma polymerised allyl alcohol (ppAOH) the power was 100 W.

3.3.2. Crystallisation Protocol for Tetragonal HEWL Crystals– Method IV

HEWL crystallisation was performed on a VDX 24 well crystallisation plate, obtained from Hampton Research, using the sitting drop vapour diffusion technique. Dow Corning vacuum grease was also purchased from Hampton Research. The protocol for preparing the protein and buffer solutions is described in section 3.1.4. All manual pipetting was conducted on an open lab bench. 500 µl of buffer was pipetted into each well. 1 µl of protein (50 mg/ml HEWL in 0.1 M sodium acetate solution at pH 4.8) and 1 µl of buffer solution were pipetted into each substrate (prepared in sections 3.3.1.1 and 3.3.1.2). The substrate was then carefully inverted and using vacuum grease it was sealed over a well. The HEWL concentration on each substrate was 25 mg/ml. For control, plain glass was also used a substrate. The crystallisation plate was incubated at 19^{o}C. Crystals formed within 24 h.

3.3.3. Crystal Imaging

Images of the crystals were obtained as described in section 3.1.9.

3.3.4. Substrate Surface Characterisation

3.3.4.1. X-Ray Photoelectron Spectroscopy

XPS analysis was performed using a spectrometer the Kratos AXIS ULTRA with a mono-chromated Al k*a* X-ray source (1486.6 eV) operated at 15 mA emission current and 10 kV anode potential. The samples were inserted into the Ultra High Vacuum (UHV) chamber for analysis at a pressure of 10^{-9} Torr. The spectrometer was used in FAT (fixed analyser transmission) mode, with pass energy of 80 eV for wide scans and pass energy 20 eV for high resolution scans. The magnetic immersion lens system allowed the area of analysis for to be defined by apertures, a 'slot' aperture of 300x700 µm for wide/survey scans and high resolution scans. The take off angle for the photoelectron analyser was 90° and acceptance angle of 30°.

Electrons emitted from the top surface were taken through an electrostatic/magnetic lens system (Hybrid lens) and a hemispherical analyser (CHA). For the non-conducting samples a charge neutraliser filament above the sample surface was used to give a flux of low energy electrons providing uniform charge neutralisation. Data analysis was carried out using CASAXPS software with Kratos sensitivity factors. The high resolution peaks were correct using the C1s scans (peaks set at 285.0 eV) to correct for any sample charging (typically 4-5 eV).

3.3.4.2. Atomic Force Microscopy (AFM)

Cover slips (Scientific Laboratory Supplies Ltd No. 2 thickness) 11 x 11 mm (cut to size) were Piranha etched and plasma treated prior to AFM. Each substrate was placed on a SPM specimen disc (Agar Scientific part No. F7003) using double sided carbon discs (Agar Scientific part No. G3347N). Tapping mode AFM was conducted using a Dimensions 3000

Atomic Force Microscope (Veeco, Sunnyvale) and a Tap300Al probe (Budget Sensors).

3.3.4.3. Water Contact Angle Measurements (WCA)

The contact angle measurements were performed using a goniometer CAM 200 (KSV Ltd, Finland). Liquid used to test the contact angle of the substrates was deionised water obtained through an ELGA purification system with a measured resistivity of 18.2 MΩ. A water droplet was placed from a needle onto the surface of the sample. The complete drop profile at the solid-air interface was evaluated using Young-Laplace fit. A manual baseline was placed on the image by the operator. The contact angle was determined as the tangent of the drop profile at the 3 phase contact point. The contact angle values obtained were the mean of the measurements taken at both sides of each water droplet. At least four droplets were placed on the same sample at different locations. A mean contact angle value was obtained for each sample.

CHAPTER 4

4. Results

4.1. Physically Adsorbed Polymers in Protein Crystallisation

4.1.1. Protein Crystallisation

Human thioredoxin and HEWL were crystallised, using the sitting drop vapour diffusion method. The sample wells of the crystallisation plates were pre-coated with polymer blend films of PAA/PVOH, PAA/PVP and PVOH/PVP at various ratios. In total, both proteins were crystallised utilising 30 different polymer surfaces, and in triplicate for reproducibility.

	PAA: PVP 1:9	PAA: PVP 2:8	PAA: PVP 3:7	PAA: PVP 4:6	PAA: PVP 5:5	PAA: PVP 6:4	PAA: PVP 7:3	PAA: PVP 8:2	PAA: PVP 9:1	Control	PAA
Large Well	- - -	- - -	- - -	- - -	- - -	- - -	- - -	- - -	- - -	√ - - - -	- - -
Small Well (control)	- - -	- - -	- - -	- - -	- - -	√ - -	√ - -	- - -	- - -	√ √ √ - -	- - -
	PAA: PVOH 1:9	PAA: PVOH 2:8	PAA: PVOH 3:7	PAA: PVOH 4:6	PAA: PVOH 5:5	PAA: PVOH 6:4	PAA: PVOH 7:3	PAA: PVOH 8:2	PAA: PVOH 9:1		PVOH
Large Well	- - -	- - -	- - -	- - -	- - -	- - -	- - -	- - -	- - -		√ - -
Small Well (control)	- - -	- - -	- - -	√ - -	√ - -	√ - -	√ √ -	√ - -	√ - -		- - -
	PVP: PVOH 1:9	PVP: PVOH 2:8	PVP: PVOH 3:7	PVP: PVOH 4:6	PVP: PVOH 5:5	PVP: PVOH 6:4	PVP: PVOH 7:3	PVP: PVOH 8:2	PVP: PVOH 9:1		PVP
Large Well	√ - -	√ - -	√ √ -	√ √ -	√ √ -	- - -	√ √ √	√ √ √	√ - -		√ √ -
Small Well (control)	√ - -	√ √ -	- - -	√ - -	√ - √	- - -	√ √ -	- - -	- - -		√ - -

Table 4.1. Table showing the occurrence of trigonal mutant human thioredoxin crystals on polymer blend films, in triplicate for reproducibility, where (√) indicates the formation of crystals and (-) indicates no crystals formed.

For thioredoxin, the trigonal crystal-inducing protocol was used. No crystals were formed in the presence of polymer blends of PAA/PVOH, and PAA/PVP. Table 4.1 summarises the occurrence of human thioredoxin crystal formation, in the presence of the different polymer blend films. Photomicrographs of sample wells containing PAA/PVOH and PAA/PVP films

showed that the protein precipitated early on in the experiment, possibly due to increased nucleation, which can lead to protein aggregation.

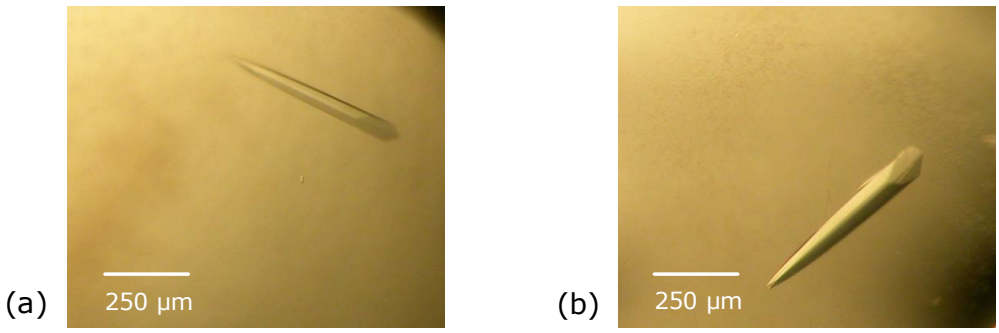

Figure 4.1. Photomicrographs showing trigonal mutant human thioredoxin crystals. Trigonal thioredoxin crystals were grown in the presence of polymer blend films and in their absence (controls). The trigonal thioredoxin crystal formed in (a) the presence of a polyvinyl pyrrolidone / polyvinyl alcohol (PVP/PVOH) blend of a 7/3 ratio, is similar in size to the thioredoxin crystal formed in (b) the control, which did not contain a polymer blend.

Thioredoxin crystals started to appear after 13 days in the PVP/PVOH containing sample wells, as well as in the control sample wells (Figure 4.1). While surface poisoning was observed on some crystals, good sized thioredoxin crystals were formed overall (>250 µm largest dimension). The reliability of these results was problematic due to the lack of thioredoxin crystals in many control wells. Overall, the results tentatively indicated to a potential use of PVP and PVOH surfaces as heterogeneous nucleants, however, the crystal growth rate was slow both in the absence and presence of PVP/PVOH polymer surfaces, as crystals formed over a 5 month period.

Further experiments concentrating on the crystallisation of thioredoxin in the presence of PVP and PVOH would be necessary, unfortunately, due to slow crystal growth rate, the mutant human thioredoxin protein was not utilised in further experiments in this research due to the time constraints of the project.

HEWL was crystallised in the presence of polymer blend films of PAA/PVP and PAA/PVOH. As the amount of PAA increased, in the composition of

both polymer blends, there was a visible effect on the HEWL crystal formation (Figure 4.2). Crystal aggregates were formed and the nucleation density of the HEWL crystals increased, as the size of the crystals decreased. Finally, in the presence of only PAA, a glut of microcrystals formed along the surface of the sample wells.

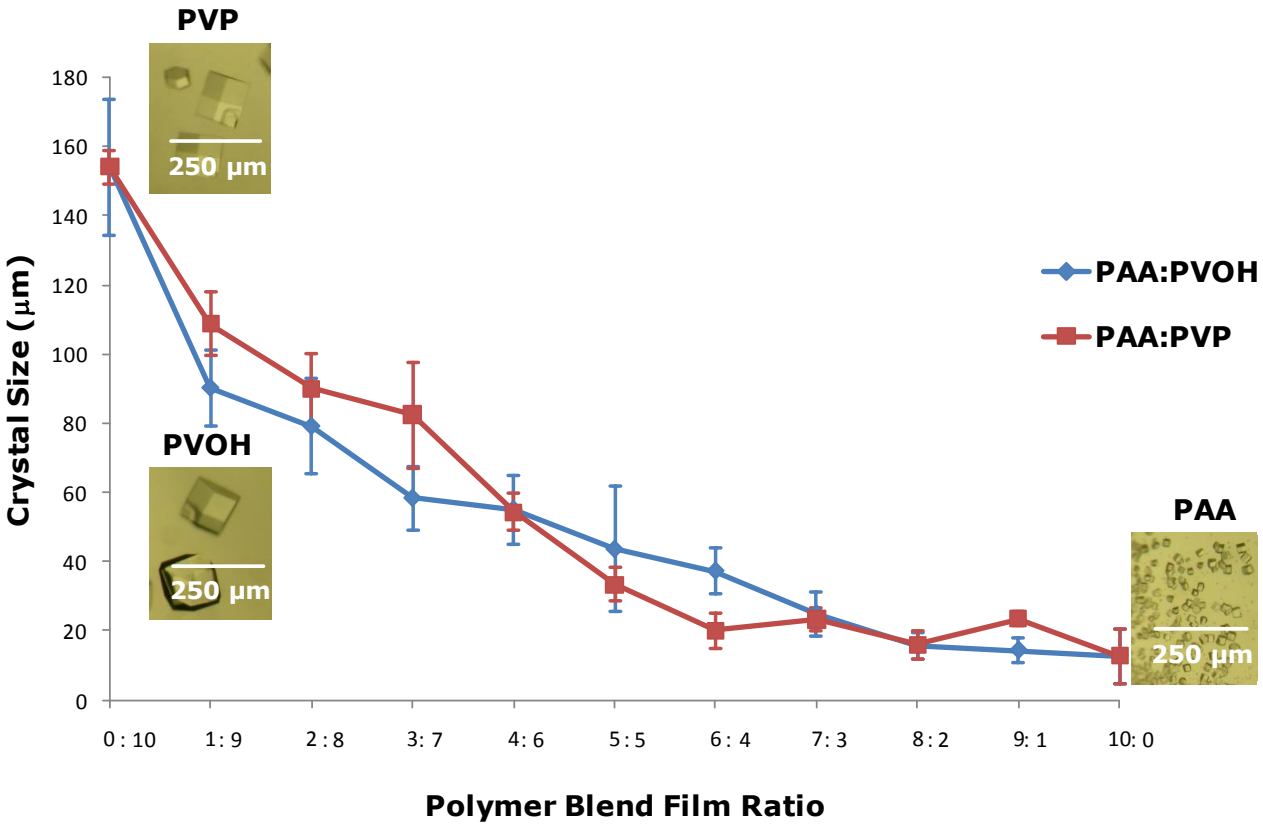

Figure 4.2. Graph showing the size of hen egg-white lysozyme (HEWL) crystals in the presence of physically adsorbed polymer blends, using the following polymers: polyacrylic acid (PAA), polyvinyl pyrrolidone (PVP) and polyvinyl alcohol (PVOH). Error bars represent mean ± standard deviation (n=3).

In contrast, HEWL crystals formed in the presence of polymer blend films made of PVP/PVOH appeared similar in size to the HEWL crystals obtained in the controls, in the absence of polymers. Some crystal surface poisoning was observed, which is the incorporation of impurities within the crystal structure, indicated by rough sections on the surfaces of the tetragonal HEWL crystals.

A solubility test showed that PAA can dissolve in the aqueous protein/buffer mixture used in the crystallisation experiments, provided that the mixture is agitated for a brief period of time. However, the crystallisation plates were not subjected to rigorous agitation and most of the HEWL crystals formed along the surface of the sample wells. This suggests that any PAA that remained in film form could have acted as a heterogeneous nucleant to the HEWL crystals, which were in contact with sample well surfaces.

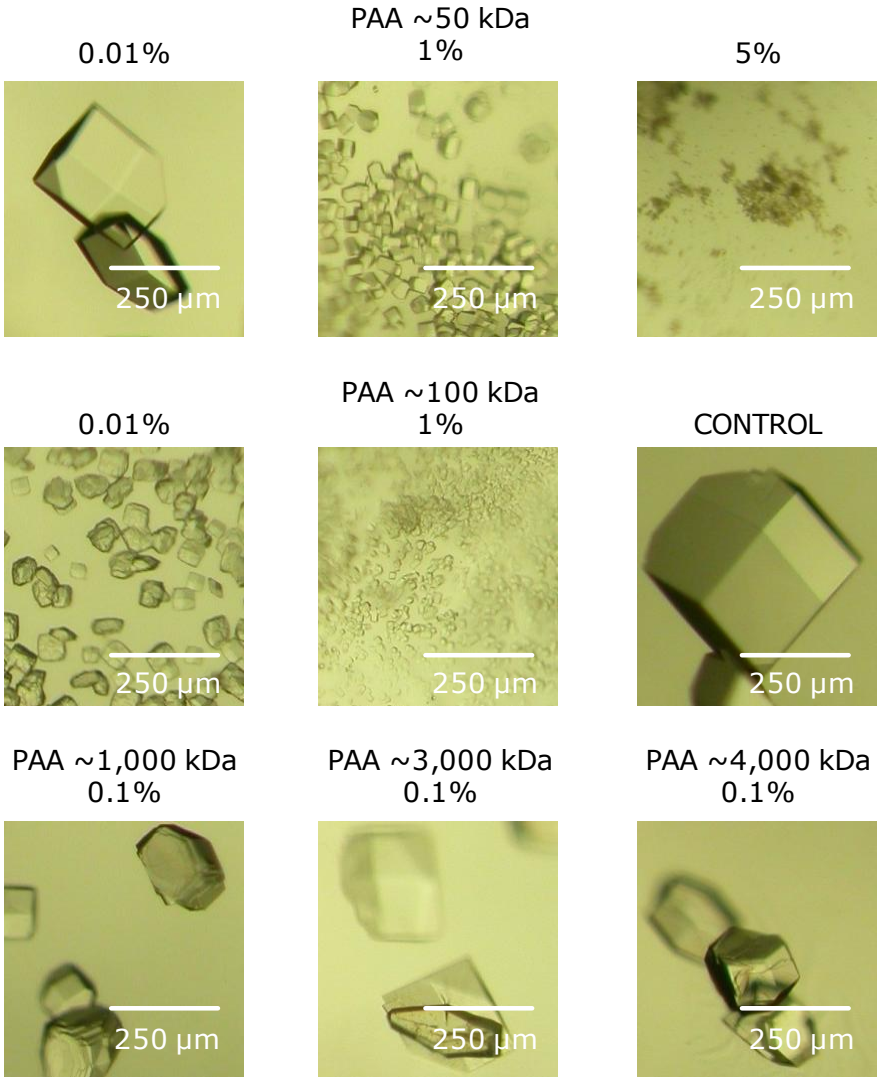

Figure 4.3. Photomicrographs of hen egg-white lysozyme (HEWL) crystals grown in the presence of adsorbed polyacrylic acid (PAA) (casting solution concentrations).

In order to further observe the effect of PAA on HEWL crystallisation, higher molecular weight PAA was used (from ~50 kDa to ~4,000 kDa) and films of increasing concentration were created (Figure 4.3). Given the PAA solubility in the protein/buffer HEWL crystallisation mixture, the increased molecular weight and concentration should have allowed for the majority of the PAA to remain in film form for a longer time, so it could act as a heterogeneous nucleant during HEWL crystallisation.

Tetragonal HEWL crystals formed throughout the protein-buffer solution contained within the wells, in the presence of PAA ~50 kDa films created by low casting concentration solutions (0.01% and 0.1%), and were similar to the ones obtained in the controls, in the absence of PAA. As the concentration of PAA increased, the number of crystals formed increased, the crystal size decreased to a few μm; and aggregates of microcrystals were observed. Crystals were formed only at the surface of the sample wells, suggesting that, PAA films were acting as heterogeneous nucleants, lowering the nucleation energy barrier, resulting in the growth of multiple tetragonal HEWL microcrystals. Finally at polymer casting solution concentrations of 3.5% to 5%, HEWL precipitated out of solution. A similar effect was observed when PAA ~100 to ~4,000 kDa was used.

4.1.2. X-ray Crystallography

While cross polar microscopy confirmed that the crystals formed in the above mentioned experiments were protein crystals and not salt crystals, x-ray crystallography was also conducted on crystal samples in order to confirm that the crystallisation experiments yielded the desired results.

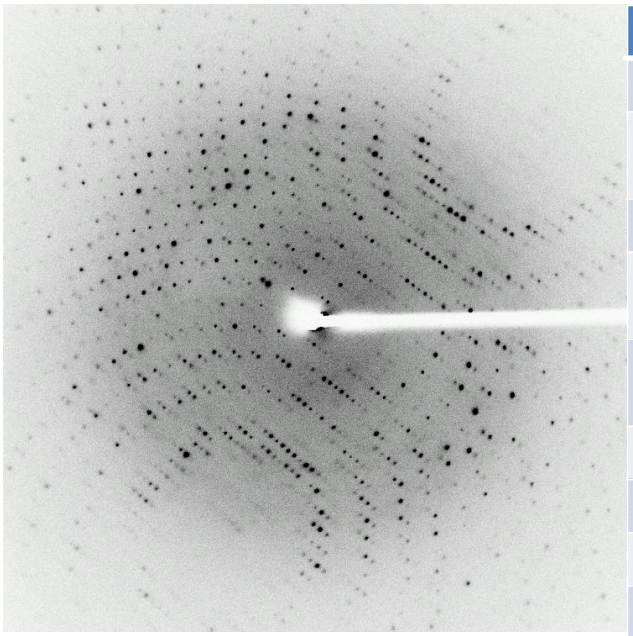

Summary of Data Collection Statistics	
Space group	$P3_121$
Unit cell dimensions	62.11 Å 62.11 Å 90.68 Å 90.00˚ 90.00˚ 120.00˚
Resolution range (Å)	26.35 – 1.78
Total number of reflections	58281
Number of unique reflections	19880
Average redundancy	2.93
Completeness (%)	99.7
Rmerge	0.043
Reduced Chi Squared	0.96

Figure 4.4. Diffraction pattern and summary of data collection statistics yielded by a single thioredoxin crystal.

Figure 4.4 and Figure 4.5 illustrate the diffraction patterns of thioredoxin and HEWL crystals obtained following x-ray crystallography.

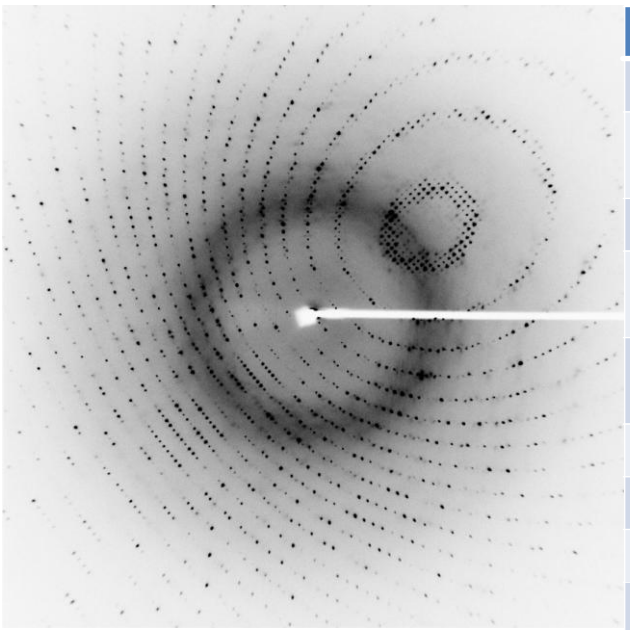

Summary of Data Collection Statistics	
Space group	$P4_32_12$
Unit cell dimensions	78.60 Å 78.60 Å 36.93 Å 90.00˚ 90.00˚ 90.00˚
Resolution range (Å)	21.37 – 1.78
Total number of reflections	62933
Number of unique reflections	11554
Average redundancy	5.45
Completeness (%)	99.9
Rmerge	0.030
Reduced Chi Squared	0.99
Output (I/sigI)	38.1

Figure 4.5. Diffraction pattern and summary of data collection statistics yielded by a single hen egg-white lysozyme (HEWL) crystal.

4.2. Polymers as Precipitants in Protein Crystallisation

4.2.1. Protein Crystallisation

The next step was to compare HEWL crystallisation in the presence of PAA in solution, acting as a precipitant, by dissolving PAA within the buffer mixture used in the crystallisation of HEWL (Figure 4.6). The size of the crystals in the presence of PAA in solution decreased and the nucleation density increased. However, these effects were not as pronounced as when PAA films were used during HEWL crystallisation, which resulted in multiple microcrystals being formed. In addition, a different form of HEWL crystals, that of needles with a 'sea-urchin' morphology, formed at PAA concentrations of 5% to 6%, in solution. This morphology of HEWL has been previously reported (94, 95).

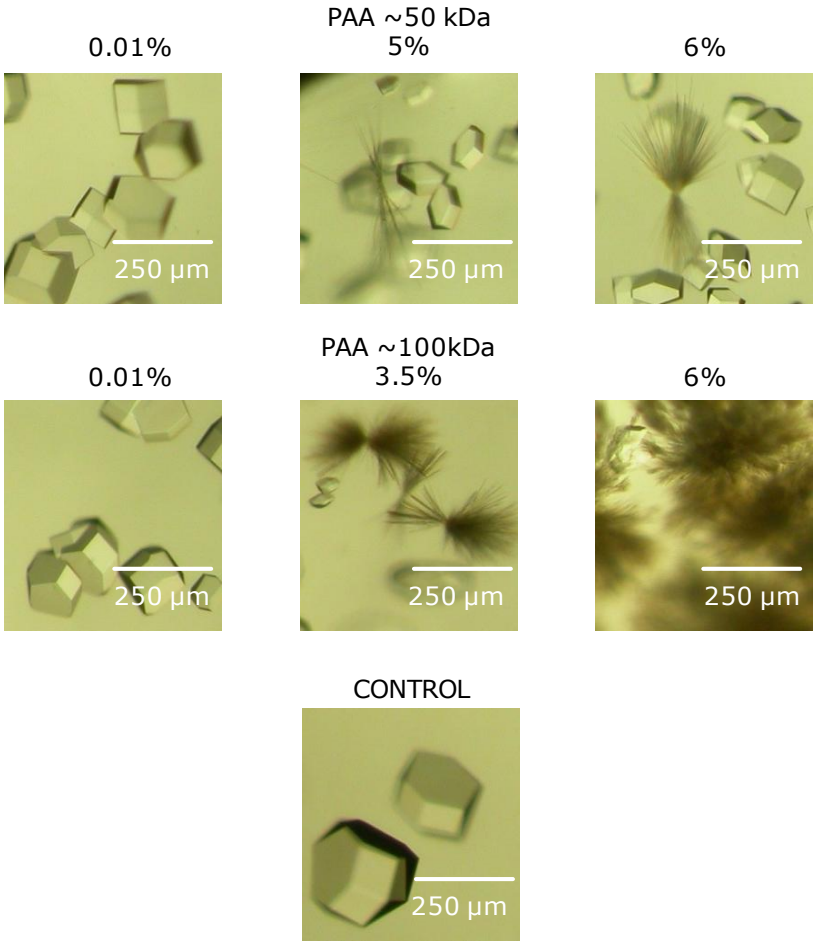

Figure 4.6. Photomicrographs of hen egg-white lysozyme (HEWL) crystals grown in the presence of polyacrylic acid (PAA) in solution as a precipitant (solution concentrations).

A similar effect on HEWL crystallisation was observed when PAA ~100 kDa was present in solution. PAA concentrations of 3.5% to 6% resulted in concomitant formation of needle and tetragonal HEWL crystals, with reproducible (i.e. within all the sample wells) needle crystal growth at high concentrations. Overall, PAA in solution, at relatively high concentrations, resulted in the growth of a different HEWL crystal form. Needle crystals formed at a slower rate than tetragonal crystals. Specifically, tetragonal crystals grew within 24 h, while needle crystals grew within 4 days. Needle crystal growth was more reproducible at high concentrations, when PAA ~100 kDa was present in solution.

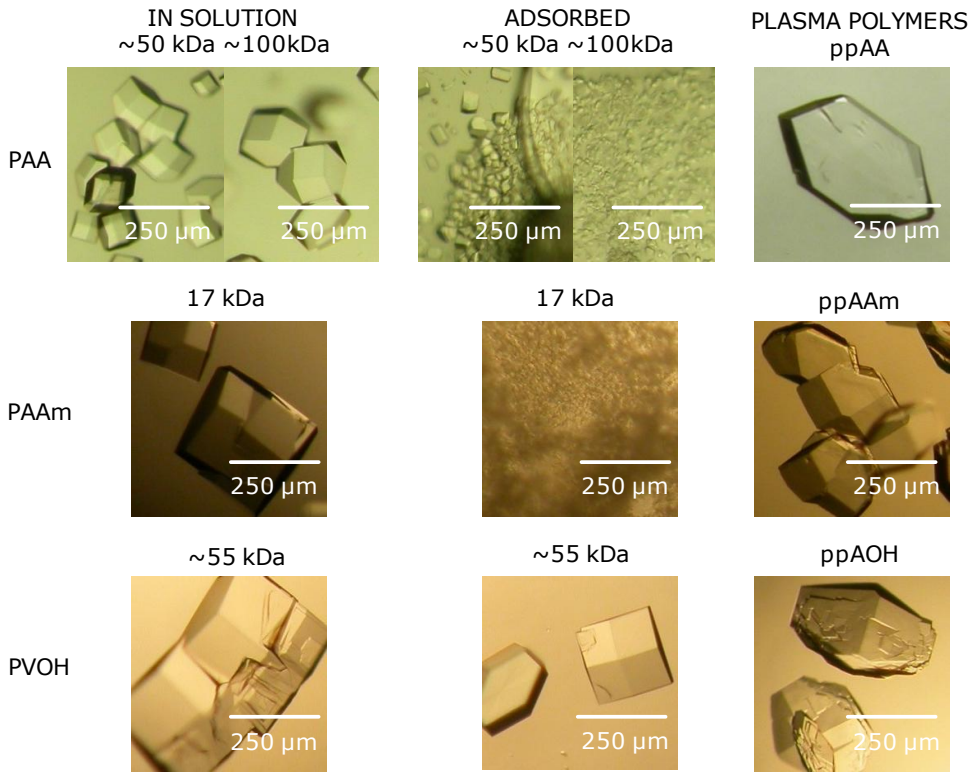

Figure 4.7. Photomicrographs of hen egg-white lysozyme (HEWL) crystals grown in the presence of polymers. Polymers used include polyacrylic acid (PAA), polyallylamine (PAAm) and polyvinyl alcohol (PVOH), in solution (1% solution concentration), physically adsorbed (1% casting solution concentration), and plasma polymerised acrylic acid (ppAA), allylamine (ppAAm) and allyl alcohol (ppAOH). Hydrochloric acid was added in PAAm; and potassium hydroxide was added in PVOH, in solution, in order to change the pH to 4.8 which was required for HEWL crystallisation.

HEWL was also crystallised in the presence of polyallylamine (PAAm) and PVOH, in solution and as physically adsorbed films (Figure 4.7). PAAm has

a pH of 11.58 and it is soluble in aqueous solutions such as the protein-buffer mixture used in the crystallisation of HEWL. As the polymer redissolved it changed the pH of the protein-buffer mixture from 4.8 to a more basic pH, causing the protein to precipitate instantly. PAAm was also used in solution, without altering its pH, and it caused the protein to precipitate.

However, when the pH of PAAm was altered to 4.8; by utilising a pH electrode and gradually adding hydrochloric acid, it created a cationic polyelectrolyte. The PAAm hydrochloride salt was then used in solution during the crystallisation of HEWL and it resulted in tetragonal protein crystal formation at various depths of the crystallisation plate wells. At low solution concentrations, (0.01% and 0.1%), the HEWL crystals were the same as those formed in the controls, in the absence of PAAm. As the concentration of the salt increased the HEWL crystals showed surface poisoning. From a concentration of 2.5% and above there was a concomitant formation of tetragonal and needle HEWL crystals.

PVOH in solution and as physically adsorbed films caused surface poisoning of the tetragonal HEWL crystals. Crystals grew at various depths within the crystallisation plate wells, and the size and nucleation density of the crystals appeared unaffected. There was no concomitant formation of needle and tetragonal crystals, as the concentration of the polymer was not above 1% (both as casting solution and 'in solution' concentration).

4.3. Plasma Treated Surfaces and Protein Crystallisation

In order to avoid cast polymer films redissolving in the aqueous protein-buffer mixture, it was necessary to look for polymers that had a similar

chemical functionality to the above mentioned polymers but had an alternative mechanism of attachment. Plasma polymers are highly cross-linked and are covalently linked to the substrate surface. Figure 2.3 illustrated the preparation stages of the glass substrates prior to their plasma polymerisation for the creation of heteronucleant polymer substrates to be utilised in protein crystallisation.

4.3.1. Water Contact Angle

Table 4.2 demonstrates how chemical treatments alter the glass substrate surface hydrophilicity. Piranha etching, resulted in a highly hydroxylated surface which is very hydrophilic. Oxygen etching further decreased the θ angle measured, where as the WCA measurements for each of the plasma polymerised surfaces matched previously recorded data (96) and were less hydrophilic.

	Unclean cover slip	Acetone washed cover slip	Piranha etched cover slip	Oxygen etched cover slip	ppAcrylic acid	ppAllylamine	ppAllyl alcohol
Mean contact angle	61.16°	67.78°	19.44°	17.86°	73.67°	71.59°	79.55°
Standard deviation (±)	3.65°	1.26°	0.51°	1.52°	1.42°	1.03°	1.27°

Table 4.2. Table containing Water Contact Angle (WCA) measurement of glass surfaces at various stages during the preparation of plasma polymerised substrates.

4.3.2. Atomic Force Microscopy

The topography of the glass substrates was also measured at the same stages as section 4.3.1, during their preparation prior to their use in protein crystallisation, following plasma polymer deposition. A sample of AFM micrographs illustrating the changes in topography, especially following the Piranha etching treatment, can be seen in Figure 4.8.

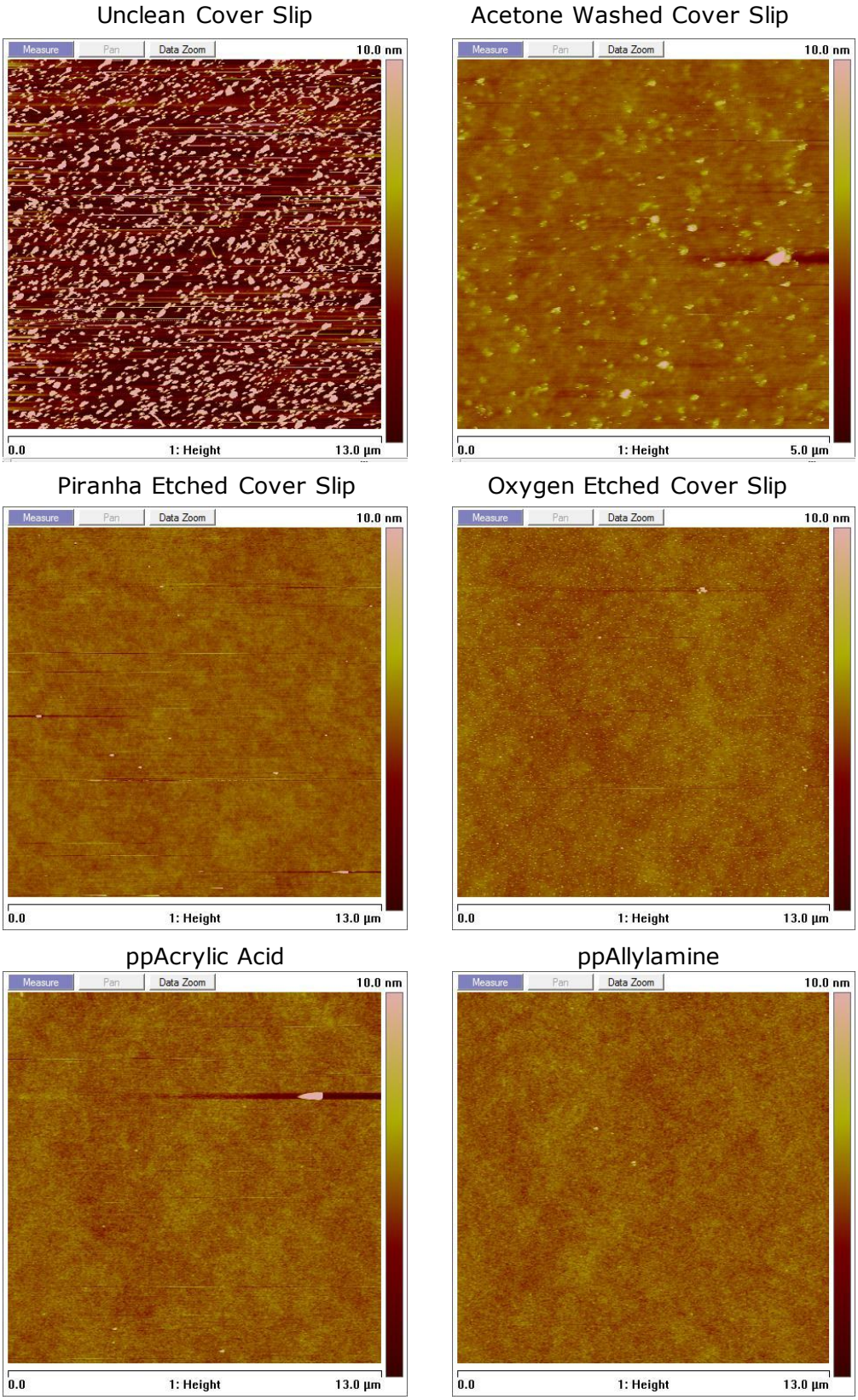

Figure 4.8. Atomic Force Microscopy (AFM) micrographs of unclean glass (coverslip), acetone washed glass, piranha etched glass, oxygen etched glass, plasma polymerised acrylic acid (ppAA) and plasma polymerised allylamine (ppAAm) glass.

4.3.3. X-ray Photoelectron Spectroscopy

Both wide survey and high resolution scans were obtained of sample surfaces at the same preparation stages as those in sections 4.3.1 and 4.3.2. The full set of data can be seen in appendix A.

4.3.4. Protein Crystallisation

Plasma polymerised acrylic acid (ppAA), allylamine (ppAAm) and allyl alcohol (ppAOH) were prepared and used in the crystallisation of HEWL (Figure 4.7). Due to the preparation of the plasma treated surfaces, it was necessary to use hanging drop vapour crystallisation instead of the sitting drop vapour diffusion method used so far in the crystallisation of HEWL.

The HEWL crystals formed on all surfaces were visible under a stereomicroscope (section 3.1.9) and were of uniform size (Figure 4.7). However, the use of ppAOH caused surface poisoning of the HEWL crystals. The crystals were similar in size to the ones formed in the absence of polymers (~250-270 μm largest dimension), with clusters of HEWL crystals also observed in the presence of ppAOH (Figure 4.9). In contrast, no surface poisoning was observed in the presence of ppAAm. However, crystal nucleation was affected, with large numbers of crystal clusters forming in the presence of ppAAm.

Crystal clustering is observed when various surfaces were used, such as plain glass as well as cleaned glass (acetone washed, Piranha and oxygen etched glass). In comparison, ppAA caused some surface poisoning but resulted in the formation of single tetragonal crystals, which are required in X-ray crystallography.

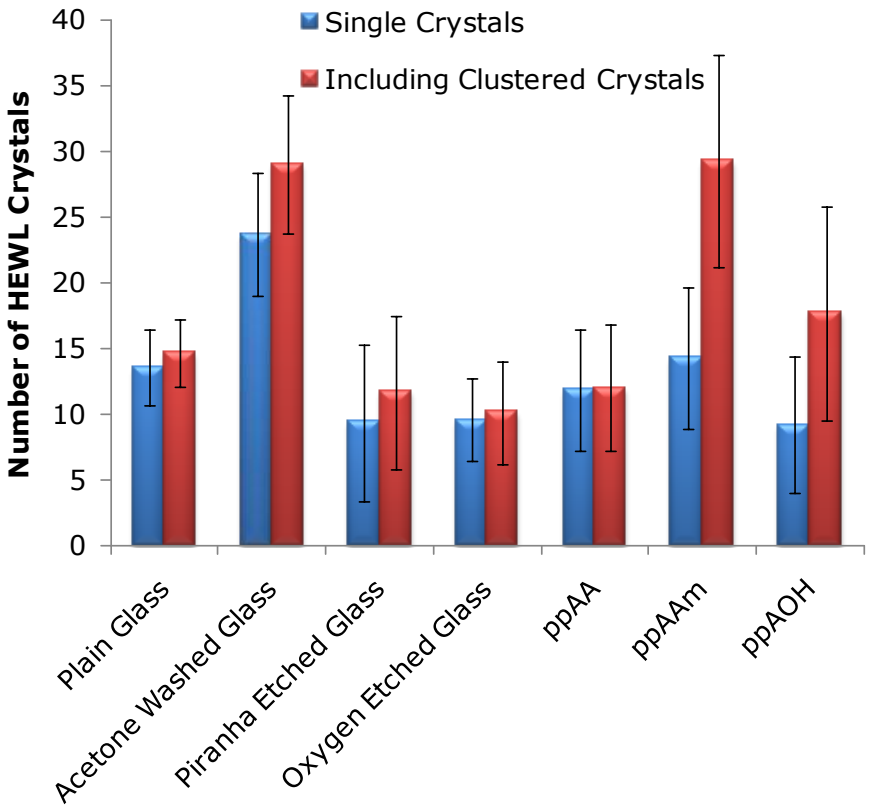

Figure 4.9. Graph showing the number of hen egg-white lysozyme (HEWL) crystals in the presence of various surfaces used in hanging drop vapour diffusion crystallisation. All HEWL crystals were visible under a stereomicroscope and had a uniform size (~250-270 μm in largest dimension). Error bars represent mean ± standard deviation (n≥3).

The ability to crystallise proteins using the minimum amount possible is advantageous, as protein purification usually yields small quantities. When the protein concentration used was lowered, ppAA did not crystallise HEWL at concentrations lower than 12 mg/ml. This agrees with published data where polymers were used as heterogeneous nucleants for HEWL (40).

Finally, an experiment was conducted in order to see the effect of surface ageing on protein crystallisation. Figure 4.10 shows how the water contact angle measurements of four different surfaces (plain, Piranha etched glass, oxygen etched glass, and ppAA), changed over a period of 5

days. The HEWL crystals appeared unaffected by the change in hydrophobicity/hydrophilicity.

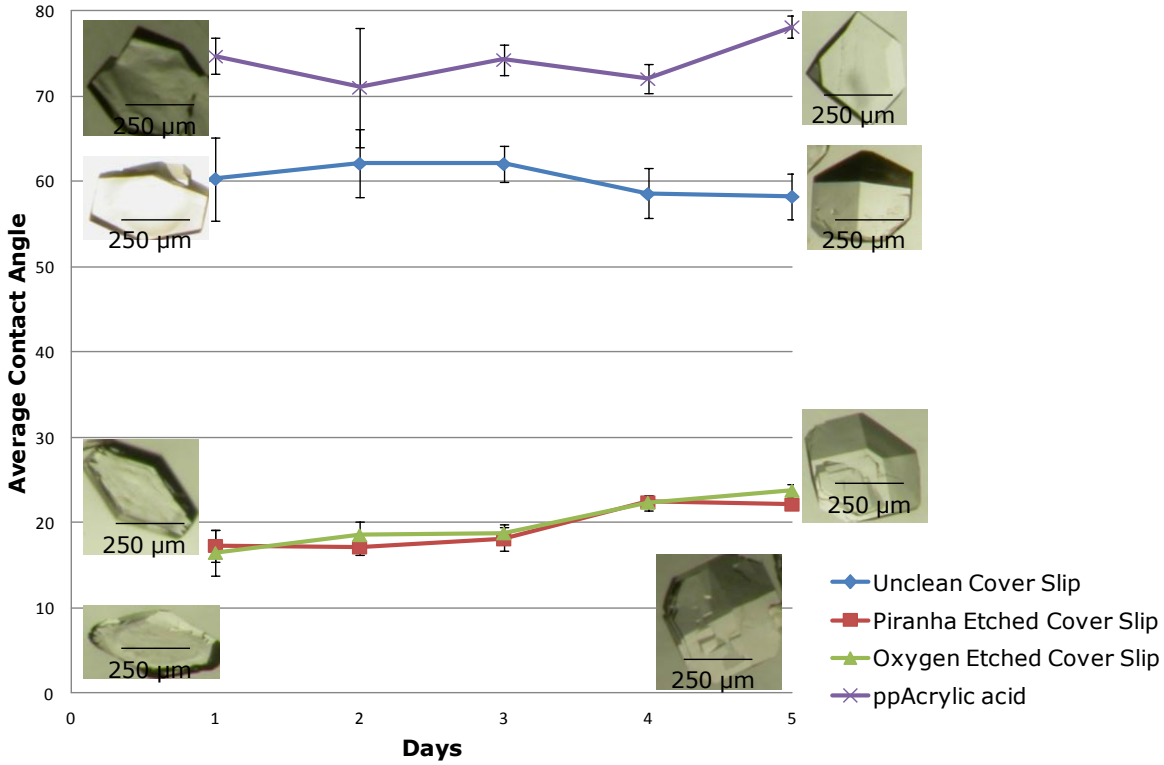

Figure 4.10. Graph showing the average water contact angle measurements of plain glass, Piranha etched and plasma treated surfaces over time. The photomicrographs of hen egg-white lysozyme (HEWL) crystals grown on the various surfaces on day 1 and on 5 days old surfaces, were included to demonstrate the uniform habit of the crystals. The HEWL crystals appeared unaffected by the hydrophobicity/hydrophilicity changes of the substrate surfaces caused by their aging. Error bars represent mean ± standard deviation (n≥4).

CHAPTER 5

5. Discussion, Conclusions and Future Applications

5.1. Discussion of Physically Adsorbed Polymers and Protein Crystallisation

The ultimate aim of this area of research is to predict and control protein crystallisation via the use of polymers as heteronucleants. A first step towards this aim was to observe the effect of polymer surfaces on the crystallisation of proteins.

The two proteins selected were HEWL and mutant human thioredoxin. HEWL crystallisation is widely studied while human thioredoxin is a slightly more challenging crystallisation system. The polymers selected, PAA, PVP and PVOH, are commercially available. In the past, PAA, PVOH and PVP have been used as polymeric precipitants in the crystallisation of proteins (93). Furthermore, PAA has been used as a precipitant (93), as well as a heterogeneous nucleant in the crystallisation of HEWL (23). In addition, PAA brush particles (97) and planar PAA brushes (98) have been known to have a high protein affinity in low ionic strength, unsaturated, protein solutions.

During this research, mutant human thioredoxin was crystallised in the presence of polymer blend films. Thioredoxin crystals formed after 13 days in the presence of PVP, followed by crystal growth in the corresponding control sample wells. Thioredoxin crystals nucleated and grew in the presence of PVP/PVOH polymer blend films and in control samples wells, in the absence of polymers. This could be due to the polymer blend films made of PVP/PVOH acting as heterogeneous nucleants. The polymer surfaces could potentially have lowered the energy barrier that prevents the ordered aggregation of macromolecules,

and induced the formation of ordered thioredoxin crystal nuclei, by adsorbing the protein molecules. The partially immobilised protein molecules could have then formed ordered intermolecular interactions resulting in crystal nuclei.

While reproducibility of the results is not ideal, as crystals did not form in all the controls, the crystal growth rate was slow both in the absence and presence of PVP/PVOH polymer surfaces, as crystals formed over a 5 month period. However, the results indicated that the thioredoxin crystal nucleation rate was increased in the presence of PVOH and PVP. In general, nucleation that occurs at a faster rate, than in the absence of a polymer film, but has a growth rate which results in large crystals (>250 μm largest dimension) suitable for X-ray diffraction analysis, is a desirable effect and bears further investigation.

When considering the HEWL crystallisation results, microcrystal formation in the presence of PAA films could have been due to an increased number of nucleation sites forming, which in turn affects the size and quality of the crystals, as there is an inverse correlation between size and nucleation density. The average size of tetragonal HEWL crystals was over 250 μm when 20 or less nucleation sites were formed. Inversely, multiple nucleation sites commonly resulted in smaller crystals.

Overall, the nucleation appeared to be more affected by the presence of PAA, than by PVP and/or PVOH films. It has been reported that, crystal formation under low-ionic strength conditions appears to proceed to completion more rapidly (99).

Rapid crystallisation tends to result in smaller crystals. At pH 4.8, PAA is almost non-ionic, with only partially deprotonated carboxylate groups, while lysozyme has a positive net charge (100). Provided that PAA, which

is soluble in water, partially redissolved in the crystallisation solution, it could have lowered the dielectric constant of the solution, resulting in an increase of the effective distance over which protein electrostatic effects occurred, leading to protein aggregation and the formation of multiple crystal nuclei.

Moreover, ionic interactions between the partially deprotonated carboxylate groups of PAA (pKa 4.5) and the exposed positively charged arginines and lysines of HEWL (pI 11.35) (Figure 1.5), at pH 4.8, may have led to anchoring of the HEWL molecules by the PAA film. This can result in the formation of multiple nucleation sites, supporting the formation of multiple microcrystals.

PAA films of high concentrations appeared to have caused protein molecules to immediately separate in the supersaturated solution and form kinetically favoured amorphous aggregates. The increased aggregation rate would have prevented the slow formation of ordered intermolecular interactions, which would have led to crystal nuclei formation and crystal growth.

5.2. Discussion of Polymers as Precipitants and Protein Crystallisation

PAA in solution acted as a precipitant and not as a heterogeneous nucleant, as crystals formed at different depths within the wells of the crystallisation plate, in comparison to the formation of crystals along the bottom of the wells in the presence of PAA films. Polymers, such as PEG, are often used in protein crystallisation experiments. PAA and PAAm, as precipitants in solution at high concentrations, may have caused a 'salting out' effect during HEWL crystallisation. This occurs when the ionic

strength is increased to the point where salt ions and protein molecules compete for solvent/water molecules to maintain their hydration layers and therefore their solubility. To fulfil their electrostatic requirements, the protein molecules begin to self-associate (18). This 'salting out' effect can explain the growth of a different HEWL crystal form, that of needles, in the presence of PAA and PAAm in solution.

HEWL needle crystals have been previously observed under chloride (23, 101), nitrate and thiocyanate (102) salt conditions. In previous studies, this form of crystals has been grown in solutions with high salt concentrations (101, 102), and in the presence of acid-functionalised polymeric surfaces, such as cross-linked acrylic acid and methacrylic acid (23). The growth rate of needle crystals is slower than that of tetragonal HEWL crystals. The increased nucleation sites caused by the high concentration of precipitant in combination with the increased viscosity of these solutions, may have promoted the formation and growth of HEWL needle crystals. This is supported by the formation of needle crystals in the presence of PAA ~50 kDa, ~100 kDa and PAAm, at high 'in solution' concentrations.

5.3. Discussion of Plasma Treated Surfaces and Protein Crystallisation

The precipitation of HEWL in the presence of PAAm films was caused by the film redissolving in the solution and increasing the pH above the optimum levels, which are between pH 4.3 to 4.8. Basic proteins, such as HEWL (pI 11.35) crystallise 0.5-3 pH units below their pI point while extreme values of pH do not contribute significantly to the successful crystallisation of proteins (17, 24). When using ppAAm there was crystal

clustering with molecules being improperly ordered within the crystal lattice, leading to defects. A possible way to avoid those clusters is to use a lower protein concentration during protein crystallisation.

PVOH and ppAOH did not appear to affect protein crystallisation, aside from surface poisoning, which is where an impurity or foreign particle is incorporated within the crystal. The impurity in turn improperly fits the crystal lattice and impacts the disposition of neighbouring molecules, which in turn produces strain that is subsequently propagated through the lattice (14).

ppAA has been shown to favour single crystal growth. In contrast to the partially deprotonated PAA films, the highly cross-linked plasma polymer had ester and ether groups due to the nature of the plasma polymer deposition (see Appendix A). Thus it had a reduced ability to act as a hydrogen donor to the positively charged HEWL, which may explain why there were fewer nucleation sites, resulting in the formation of large single crystals. Some deprotonated carboxyl groups of ppAA may have aided in HEWL crystallisation but the effect was not the same as when PAA was in the form of physically adsorbed films.

Finally, it appears that drop shape, as indicated by the water contact angles of Figure 4.10, had no major effect to the crystallisation of HEWL. However, there is a possibility that growth rate may have been affected, though the crystal habit of HEWL appeared to be consistent with those formed in the controls.

5.4. Conclusions and Future Applications

The hypothesis of this work was that polymers can direct crystal habit and polymorphism. The data presented here have shown that physically adsorbed PAA can direct crystal habit formation, while PAA and PAAm, as precipitants in solution at high concentrations, may have caused a 'salting out' effect during HEWL crystallisation resulting in the growth of a different form of HEWL crystal.

The data presented here agree with published work where PAA, PVOH and PVP have been used as polymeric precipitants in the crystallisation of proteins (93). Furthermore, PAA has been used as a precipitant (93), as well as a heterogeneous nucleant in the crystallisation of HEWL (23). In addition, PAA brush particles (97) and planar PAA brushes (98) have been known to have a high protein affinity in low ionic strength, unsaturated, protein solutions.

Future work could involve the creation of brushes, grafted from surfaces, with various functional groups such as carboxyl groups, their characterisation and use in protein crystallisation. The ultimate goal would be to utilise protein-imprinted polymers as heteronucleants to a vast array of proteins, including membrane proteins which are difficult to crystallise. Detailed characterisation of those imprinted surfaces would aid in better understanding the mechanisms at work behind the already successful crystallisation work recently published (56, 83) in the area of polymer mediated protein crystallisation.

REFERENCES

1. J. Fiaux, E.B. Bertelsen, A.L. Horwich, and K. Wuthrich. NMR analysis of a 900K GroEL-GroES complex. Nature. 418:207-211 (2002).
2. B. Shaanan. Structure of human oxyhaemoglobin at 2.1 A resolution. Journal of Molecular Biology. 171:31-59 (1983).
3. Z. Kam, H.B. Shore, and G. Feher. Crystallization of Proteins. Journal of Molecular Biology. 123:539-555 (1978).
4. H.M. Berman, J. Westbrook, Z. Feng, G. Gilliland, T.N. Bhat, H. Weissig, I.N. Shindyalov, and P.E. Bourne. The Protein Data Bank. Nucleic Acids Research. 28:235-242 (2000).
5. T. Pham, D. Lai, D. Ji, W. Tuntiwechapikul, J.M. Friedman, and T.R. Lee. Well-ordered self-assembled monolayer surfaces can be used to enhance the growth of protein crystals. Colloids and Surfaces, B: Biointerfaces. 34:191-196 (2004).
6. R. Capdeville, E. Buchdunger, J. Zimmermann, and A. Matter. Glivec (STI571, imatinib), a rationally developed, targeted anticancer drug. Nature Reviews Drug Discovery. 1:493-502 (2002).
7. S.H. Choi, J.H. Kwon, and C.W. Kim. Microencapsulation of insulin microcrystals. Bioscience, Biotechnology, and Biochemistry. 68:749-752 (2004).
8. M.J. Mizianty and L. Kurgan. Sequence-based prediction of protein crystallization, purification and production propensity. Bioinformatics. 27:i24-i33 (2011).
9. R. Cudney, S. Patel, K. Weisgraber, Y. Newhouse, and A. McPherson. Screening and optimization strategies for macromolecular crystal growth. Acta Crystallographica, Section D: Biological Crystallography. 50:414-423 (1994).
10. I.F. Roberts. Crystals and their Structures, Methuen Educational Ltd, London, 1974.
11. Introduction to Minerals and Crystals, The Natural History Museum, London, 2008.
12. P.C. Weber. Physical principles of protein crystallization. Advanced Protein Chemistry. 41:1-36 (1991).
13. G. Feher and Z. Kam. Nucleation and growth of protein crystals: general principles and assays. Methods in Enzymology. 114:77-112 (1985).
14. A. McPherson. Crystallization of Biological Macromolecules, Cold Spring Harbor Laboratory Press, New York, 1999.
15. R. Boistelle and J.P. Astier. Crystallization mechanisms in solution. Journal of Crystal Growth. 90:14-30 (1988).
16. S. Koszelak, D. Martin, J. Ng, and A. McPherson. Protein crystal growth rates determined by time lapse microphotography. Journal of Crystal Growth. 110:177-181 (1991).
17. N.E. Chayen, J.R. Helliwell, and E.H. Snell. Macromolecular Crystallization and Crystal Perfection, Oxford University Press, New York, 2010.
18. D.Y. Chirgadze. Protein Crystallisation in Action, University of Cambridge, 2001.
19. N.E. Chayen. Comparative studies of protein crystallization by vapour-diffusion and microbatch techniques. Acta

Crystallographica, Section D: Biological Crystallography. 54:8-15 (1998).

20. J.R. Luft and G.T. DeTitta. Kinetic aspects of macromolecular crystallization. Methods in Enzymology. 276:110-131 (1997).

21. T. Beyer, G.M. Day, and S.L. Price. The prediction, morphology, and mechanical properties of the polymorphs of paracetamol. Journal of the American Chemical Society. 123:5086-5094 (2001).

22. M.L. Peterson, S.L. Morissette, C. McNulty, A. Goldsweig, P. Shaw, M. LeQuesne, J. Monagle, N. Encina, J. Marchionna, A. Johnson, J. Gonzalez-Zugasti, A.V. Lemmo, S.J. Ellis, M.J. Cima, and O. Almarsson. Iterative high-throughput polymorphism studies on acetaminophen and an experimentally derived structure for form III. Journal of the American Chemical Society. 124:10958-10959 (2002).

23. A.L. Grzesiak and A.J. Matzger. Selection of protein crystal forms facilitated by polymer-induced heteronucleation. Crystal Growth & Design. 8:347-350 (2008).

24. A. Ducruix and R. Giege. Crystallization of Nucleic Acids and Proteins. A Practical Approach, Oxford University Press, New York, 1992.

25. R. Boistelle, J.P. Astier, G. Marchis-Mouren, V. Desseaux, and R. Haser. Solubility, phase transition, kinetic ripening and growth rates of porcine pancreatic alpha-amylase isoenzymes. Journal of Crystal Growth. 123:109-120 (1992).

26. B. Cudney and S. Patel. Crystallization as a tool for bioseparation. American Biotechnology Laboratory. 12:42 (1994).

27. N.E. Chayen. The role of oil in macromolecular crystallization. Structure. 5:1269-1274 (1997).

28. A.A. Chernov. Crystal growth and crystallography. Acta Crystallographica, Section A: Foundations of Crystallography. 54:859-872 (1998).

29. J.M. Garcia-Ruiz. Nucleation of protein crystals. Journal of Structural Biology. 142:22-31 (2003).

30. A. McPherson, A.J. Malkin, Y.G. Kuznetsov, and M. Plomp. Atomic force microscopy applications in macromolecular crystallography. Acta Crystallographica, Section D: Biological Crystallography. 57:1053-1060 (2001).

31. M. Ataka. Protein crystal growth: An approach based on phase diagram determination. Phase Transitions. 45:205-219 (1993).

32. G. Rhodes. Crystallography Made Crystal Clear: A Guide for Users of Macromolecular Models Academic Press, Inc., London, 1993.

33. C.N. Nanev. Protein crystal nucleation: Recent notions. Crystal Research and Technology. 42:4-12 (2007).

34. A. D'Arcy, A. Mac Sweeney, and A. Haber. Using natural seeding material to generate nucleation in protein crystallization experiments. Acta Crystallographica, Section D: Biological Crystallography. 59:1343-1346 (2003).

35. A. D'Arcy, A. Mac Sweeney, and A. Habera. Modified microbatch and seeding in protein crystallization experiments. Journal of Synchrotron Radiation. 11:24-26 (2004).

36. **I. Nederlof, R. Hosseini, D. Georgieva, J. Luo, D. Li, and J.P. Abrahams. A straightforward and robust method for introducing human hair as a nucleant into high throughput crystallization trials. Crystal Growth & Design. 11:1170-1176 (2011).**
37. **S. Koszelak and A. McPherson. Time lapse microphotography of protein crystal growth using a color VCR. Journal of Crystal Growth. 90:340-343 (1988).**
38. **A.A. Chernov. Modern Crystallography III, Springer, Berlin, 1984.**
39. **A.J. Malkin, J. Cheung, and A. McPherson. Crystallization of satellite tobacco mosaic virus I. Nucleation phenomena. Journal of Crystal Growth. 126:544-554 (1993).**
40. **S. Fermani, G. Falini, M. Minnucci, and A. Ripamonti. Protein crystallization on polymeric film surfaces. Journal of Crystal Growth. 224:327-334 (2001).**
41. **G. Falini, S. Fermani, G. Conforti, and A. Ripamonti. Protein crystallisation on chemically modified mica surfaces. Acta Crystallographica, Section D: Biological Crystallography. 58:1649-1652 (2002).**
42. **F.V. Hodzhaoglu and C.N. Nanev. Heterogeneous versus bulk nucleation of lysozyme crystals. Crystal Research and Technology. 45:281-291 (2010).**
43. **P. Asanithi, E. Saridakis, L. Govada, I. Jurewicz, E.W. Brunner, R. Ponnusamy, J.A.S. Cleaver, A.B. Dalton, N.E. Chayen, and R.P. Sear. Carbon-nanotube-based materials for protein crystallization. ACS Applied Materials & Interfaces. 1:1203-1210 (2009).**
44. **M.D. Lang, A.L. Grzesiak, and A.J. Matzger. The use of polymer heteronuclei for crystalline polymorph selection. Journal of the American Chemical Society. 124:14834-14835 (2002).**
45. **C.P. Price, A.L. Grzesiak, and A.J. Matzger. Crystalline polymorph selection and discovery with polymer heteronuclei. Journal of the American Chemical Society. 127:5512-5517 (2005).**
46. **A.L. Grzesiak and A.J. Matzger. New form discovery for the analgesics flurbiprofen and sulindac facilitated by polymer-induced heteronucleation. Journal of Pharmaceutical Sciences. 96:2978-2986 (2007).**
47. **A.R. Liberski, G.J. Tizzard, J.J. Diaz-Mochon, M.B. Hursthouse, P. Milnes, and M. Bradley. Screening for polymorphs on polymer microarrays. Journal of Combinatorial Chemistry. 10:24-27 (2008).**
48. **W.W. Porter, S.C. Elie, and A.J. Matzger. Polymorphism in carbamazepine cocrystals. Crystal Growth & Design. 8:14-16 (2008).**
49. **A.L. Grzesiak and A.J. Matzger. Selection and discovery of polymorphs of platinum complexes facilitated by polymer-induced heteronucleation. Inorganic Chemistry. 46:453-457 (2007).**
50. **A.L. Grzesiak, F.J. Uribe, N.W. Ockwig, O.M. Yaghi, and A.J. Matzger. Polymer-induced heteronucleation for the discovery of new extended solids. Angewandte Chemie, International Edition in English. 45:2553-2556 (2006).**

51. A. McPherson and P.J. Shlichta. Facilitation of the growth of protein crystals by heterogeneous epitaxial nucleation. Journal of Crystal Growth. 85:206-214 (1987).

52. A. McPherson and P. Shlichta. Heterogeneous and epitaxial nucleation of protein crystals on mineral surfaces. Science. 239:385-387 (1988).

53. C.J. Leung, B.T. Nall, and G.D. Brayer. Crystallization of yeast iso-2-cytochrome c using a novel hair seeding technique. Journal of Molecular Biology. 206:783-785 (1989).

54. A.S. Thakur, G. Robin, G. Guncar, N.F.W. Saunders, J. Newman, J.L. Martin, and B. Kobe. Improved success of sparse matrix protein crystallization screening with heterogeneous nucleating agents. PLoS ONE. 2:e1091 (2007).

55. S.P. Wood, R.W. Janes, E. Sweeney, and R.A. Palmer. Crystallization of bovine pancreatic polypeptide in the presence of crystalline diglycidyl ether of bisphenol A (Araldite): epitaxy or covalent nucleation. Journal of Crystal Growth. 122:204-207 (1992).

56. E. Saridakis, S. Khurshid, L. Govada, Q. Phan, D. Hawkins, G.V. Crichlow, E. Lolis, S.M. Reddy, and N.E. Chayen. Protein crystallization facilitated by molecularly imprinted polymers. Proceedings of the National Academy of Sciences of the United States of America. 108:11081-11086 (2011).

57. N.E. Chayen, E. Saridakis, and R.P. Sear. Experiment and theory for heterogeneous nucleation of protein crystals in a porous medium. Proceedings of the National Academy of Sciences of the United States of America. 103:597-601 (2006).

58. S. Stolyarova, E. Saridakis, N.E. Chayen, and Y. Nemirovsky. A model for enhanced nucleation of protein crystals on a fractal porous substrate. Biophysical Journal. 91:3857-3863 (2006).

59. A. Sanjoh, T. Tsukihara, and S. Gorti. Surface-potential controlled Si-microarray devices for heterogeneous protein crystallization screening. Journal of Crystal Growth. 232:618-628 (2001).

60. D. Tsekova, S. Dimitrova, and C.N. Nanev. Heterogeneous nucleation (and adhesion) of lysozyme crystals. Journal of Crystal Growth. 196:226-233 (1999).

61. Y.-X. Liu, X.-J. Wang, J. Lu, and C.-B. Ching. Influence of the roughness, topography, and physicochemical properties of chemically modified surfaces on the heterogeneous nucleation of protein crystals. The Journal of Physical Chemistry B. 111:13971-13978 (2007).

62. E. Drioli, G. Di Profio, and E. Curcio. Progress in membrane crystallization. Current Opinion in Chemical Engineering. 1:178-182 (2012).

63. E. Curcio, G. Di Profio, and E. Drioli. Membrane crystallization of macromolecular solutions. Desalination. 145:173-177 (2002).

64. G. Di Profio, E. Curcio, and E. Drioli. Supersaturation control and heterogeneous nucleation in membrane crystallizers: facts and perspectives. Industrial & Engineering Chemistry Research. 49:11878-11889 (2010).

65. **G. Di Profio, C. Stabile, A. Caridi, E. Curcio, and E. Drioli. Antisolvent membrane crystallization of pharmaceutical compounds. Journal of Pharmaceutical Sciences. 98:4902-4913 (2009).**
66. **E. Drioli, E. Curcio, A. Criscuoli, and G.D. Profio. Integrated system for recovery of CaCO3, NaCl and MgSO4·7H2O from nanofiltration retentate. Journal of Membrane Science. 239:27-38 (2004).**
67. **E. Curcio, G. Di Profio, and E. Drioli. Recovery of fumaric acid by membrane crystallization in the production of L-malic acid. Separation and Purification Technology. 33:63-73 (2003).**
68. **E. Curcio, G. Di Profio, and E. Drioli. A new membrane-based crystallization technique: tests on lysozyme. Journal of Crystal Growth. 247:166-176 (2003).**
69. **G. Di Profio, E. Curcio, A. Cassetta, D. Lamba, and E. Drioli. Membrane crystallization of lysozyme: kinetic aspects. Journal of Crystal Growth. 257:359-369 (2003).**
70. **G. Di Profio, V. Grosso, A. Caridi, R. Caliandro, A. Guagliardi, G. Chita, E. Curcio, and E. Drioli. Direct production of carbamazepine-saccharin cocrystals from water/ethanol solvent mixtures by membrane-based crystallization technology. CrystEngComm. 13:5670-5673 (2011).**
71. **B. Rodriguez-Spong, C.P. Price, A. Jayasankar, A.J. Matzger, and N. Rodriguez-Hornedo. General principles of pharmaceutical solid polymorphism: a supramolecular perspective. Advanced Drug Delivery Reviews. 56:241-274 (2004).**
72. **V. Lopez-Mejias, J.W. Kampf, and A.J. Matzger. Polymer-induced heteronucleation of tolfenamic acid: structural investigation of a pentamorph. Journal of the American Chemical Society. 131:4554-4555 (2009).**
73. **K.M. Lutker and A.J. Matzger. Crystal polymorphism in a carbamazepine derivative: oxcarbazepine. Journal of Pharmaceutical Sciences. 99:794-803 (2009).**
74. **K.L.A. Chan and S.G. Kazarian. Fourier transform infrared imaging for high-throughput analysis of pharmaceutical formulations. Journal of Combinatorial Chemistry. 7:185-189 (2005).**
75. **L.M. Foroughi, Y.-N. Kang, and A.J. Matzger. Polymer-induced heteronucleation for protein single crystal growth: structural elucidation of bovine liver catalase and concanavalin A forms. Crystal Growth & Design. 11:1294-1298 (2011).**
76. **R. Hoogenboom, M.A.R. Meier, and U.S. Schubert. Combinatorial methods, automated synthesis and high-throughput screening in polymer research: past and present. Macromolecular Rapid Communications. 24:16-32 (2003).**
77. **S. Brocchini, K. James, V. Tangpasuthadol, and J. Kohn. A combinatorial approach for polymer design. Journal of the American Chemical Society. 119:4553-4554 (1997).**
78. **S. Brocchini, K. James, V. Tangpasuthadol, and J. Kohn. Structure-property correlations in a combinatorial library of degradable biomaterials. Journal of Biomedical Materials Research. 42:66-75 (1998).**
79. **C. Alexander, H.S. Andersson, L.I. Andersson, R.J. Ansell, N. Kirsch, I.A. Nicholls, J. O'Mahony, and M.J. Whitcombe.**

Molecular imprinting science and technology: a survey of the literature for the years up to and including 2003. Journal of Molecular Recognition. 19:106-180 (2006).

80. T.J. Egan, A.L. Rodgers, and T. Siele. Nucleation of calcium oxalate crystals on an imprinted polymer surface from pure aqueous solution and urine. Journal of Biological Inorganic Chemistry. 9:195-202 (2004).

81. S.M. D'Souza, C. Alexander, S.W. Carr, A.M. Waller, M.J. Whitcombe, and E.N. Vulfson. Directed nucleation of calcite at a crystal-imprinted polymer surface. Nature. 398:312-316 (1999).

82. T. Matsunaga and T. Takeuchi. Crystallized protein-imprinted polymer chips. Chemistry Letters. 35:1030-1031 (2006).

83. T. Takeuchi, D. Goto, and H. Shinmori. Protein profiling by protein imprinted polymer array. Analyst. 132:101-103 (2007).

84. H. Eklund, F.K. Gleason, and A. Holmgren. Structural and functional relations among thioredoxins of different species. Proteins. 11:13-28 (1991).

85. A. Weichsel, J.R. Gasdaska, G. Powis, and W.R. Montfort. Crystal structures of reduced, oxidized, and mutated human thioredoxins: evidence for a regulatory homodimer. Structure. 4:735-751 (1996).

86. E.S. Arner and A. Holmgren. Physiological functions of thioredoxin and thioredoxin reductase. European Journal of Biochemistry. 267:6102-6109 (2000).

87. A. Holmgren. Thioredoxin. Annual Review of Biochemistry. 54:237-271 (1985).

88. J. Qin, G.M. Clore, and A.M. Gronenborn. The high-resolution three-dimensional solution structures of the oxidized and reduced states of human thioredoxin. Structure. 2:503-522 (1994).

89. J.D. Forman-Kay, G.M. Clore, P.T. Wingfield, and A.M. Gronenborn. High-resolution three-dimensional structure of reduced recombinant human thioredoxin in solution. Biochemistry. 30:2685-2698 (1991).

90. S.K. Katti, D.M. LeMaster, and H. Eklund. Crystal structure of thioredoxin from Escherichia coli at 1.68 A resolution. Journal of Molecular Biology. 212:167-184 (1990).

91. A. Smeets, C. Evrard, M. Landtmeters, C. Marchand, B. Knoops, and J.P. Declercq. Crystal structures of oxidized and reduced forms of human mitochondrial thioredoxin 2. Protein Science. 14:2610-2621 (2005).

92. J. Wang, M. Dauter, R. Alkire, A. Joachimiak, and Z. Dauter. Triclinic lysozyme at 0.65 A resolution. Acta Crystallographica, Section D: Biological Crystallography. 63:1254-1268 (2007).

93. S. Patel, B. Cudney, and A. McPherson. Polymeric precipitants for the crystallization of macromolecules. Biochemical and Biophysical Research Communications. 207:819-828 (1995).

94. D.G. Georgieva, M.E. Kuil, T.H. Oosterkamp, H.W. Zandbergen, and J.P. Abrahams. Heterogeneous nucleation of three-dimensional protein nanocrystals. Acta Crystallographica, Section D: Biological Crystallography. 63:564-570 (2007).

95. Y. Liu, X. Wang, and C.B. Ching. Toward further understanding of lysozyme crystallization: phase diagram, protein-protein interaction, nucleation kinetics, and growth kinetics. Crystal Growth & Design. 10:548-558 (2010).

96. S. Dey, B. Kellam, M.R. Alexander, C. Alexander, and F.R.A.J. Rose. Enzyme-passage free culture of mouse embryonic stem cells on thermo-responsive polymer surfaces. Journal of Materials Chemistry. 21:6883-6890 (2011).

97. K. Anikin, C. Rocker, A. Wittemann, J. Wiedenmann, M. Ballauff, and G.U. Nienhaus. Polyelectrolyte-mediated protein adsorption: fluorescent protein binding to individual polyelectrolyte nanospheres. Journal of Physical Chemistry B. 109:5418-5420 (2005).

98. O. Hollmann and C. Czeslik. Characterization of a planar poly(acrylic acid) brush as a materials coating for controlled protein immobilization. Langmuir. 22:3300-3305 (2006).

99. K.M. Gernert, R. Smith, and D.C. Carter. A simple apparatus for controlling nucleation and size in protein crystal growth. Analytical Biochemistry. 168:141-147 (1988).

100. F. Carlsson, E. Hyltner, T. Arnebrant, M. Malmsten, and P. Linse. Lysozyme absorption to charged surfaces. A Monte Carlo study. Journal of Physical Chemistry B. 108:9871-9881 (2004).

101. V. Bhamidi, E. Skrzypczak-Jankun, and C.A. Schall. Dependence of nucleation kinetics and crystal morphology of a model protein system on ionic strength. Journal of Crystal Growth. 232:77-85 (2001).

102. M.C.R. Heijna, M.J. Theelen, W.J.P. van Enckevort, and E. Vlieg. Spherulitic growth of hen egg-white lysozyme crystals. Journal of Physical Chemistry B. 111:1567-1573 (2007).

APPENDIX A

XPS Wide Scan Spectrum of Piranha Etched Substrate

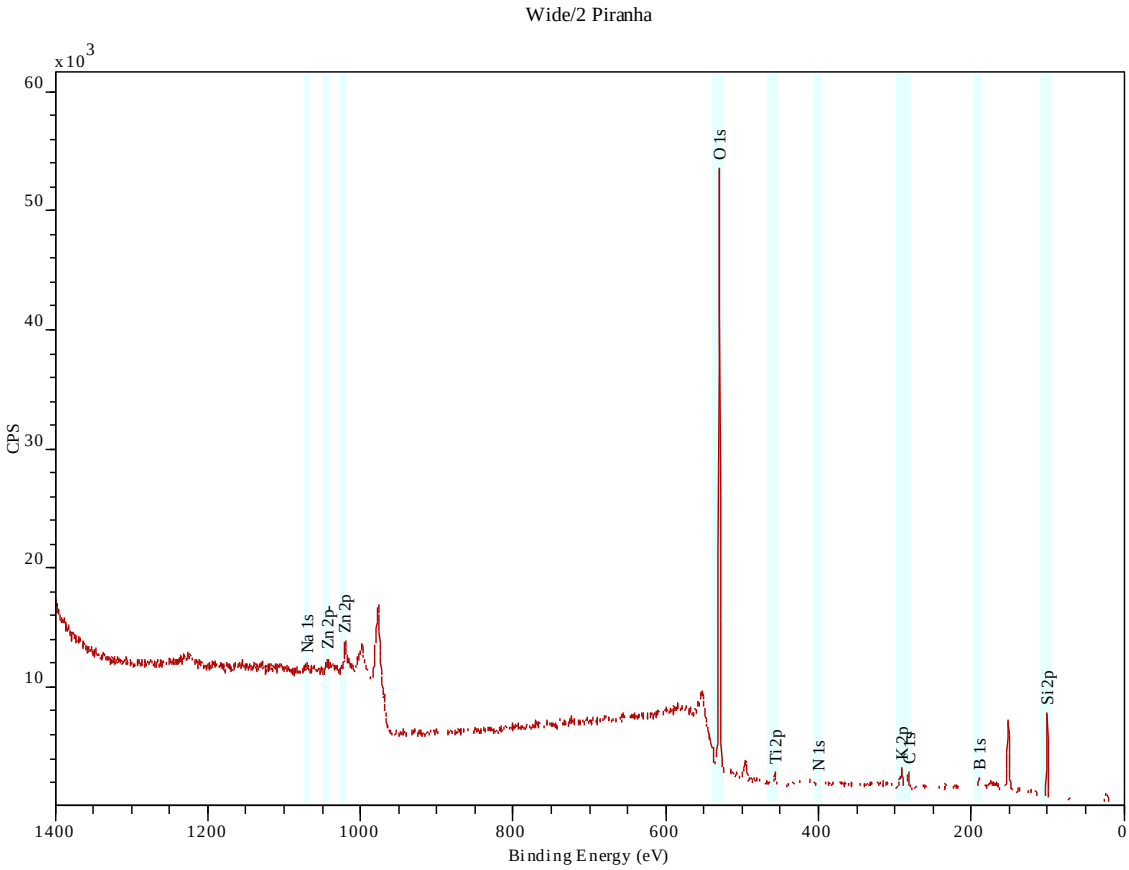

Data of Wide Scans of Piranha Etched Substrate

Electrons of Atoms Detected	Binding Energy	Atomic Percentage				
		Piranha Etched Wide Scan 1	Piranha Etched Wide Scan 2	Piranha Etched Wide Scan 3	Average of Piranha Etched Wide Scans	Standard Deviation (+/-)
Si 2p	100.0	28.54	28.76	28.84	**28.71**	**0.16**
B 1s	190.0	4.71	6.55	4.65	**5.31**	**1.08**
C 1s	282.0	4.85	3.96	6.42	**5.08**	**1.24**
K 2p	290.5	1.34	1.50	1.16	**1.34**	**0.17**
N 1s	399.5	1.02	1.14	0.61	**0.92**	**0.28**
Ti 2p	457.0	0.91	0.53	0.52	**0.65**	**0.22**
O 1s	529.5	58.10	56.85	57.04	**57.33**	**0.67**
Zn 2p	1020.0	0.29	0.30	0.30	**0.30**	**0.01**
Na 1s	1069.5	0.24	0.41	0.45	**0.37**	**0.11**

XPS Wide Scan Spectrum of Oxygen Etched Substrate

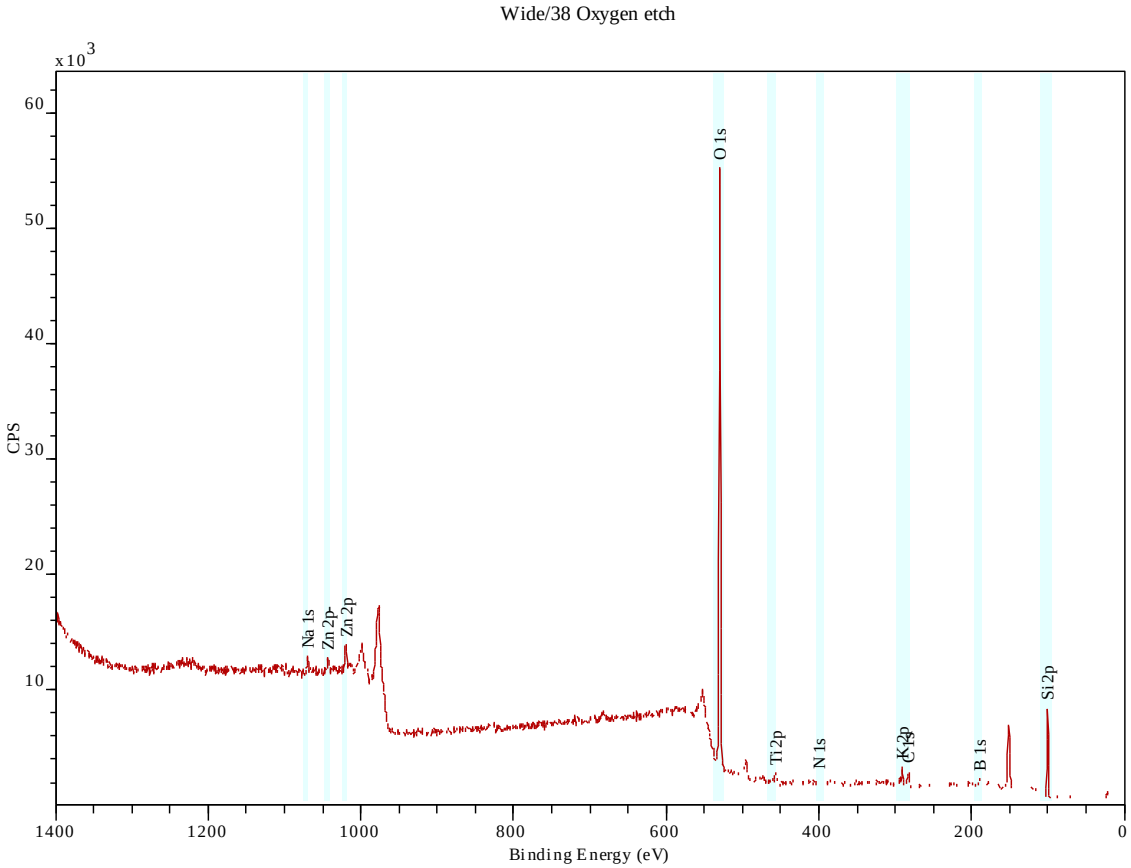

Data of Wide Scans of Oxygen Etched Substrate

Electrons of Atoms Detected	Binding Energy	Atomic Percentage				
		Oxygen Etched Wide Scan 1	Oxygen Etched Wide Scan 2	Oxygen Etched Wide Scan 3	Average of Oxygen Etched Wide Scans	Standard Deviation (+/-)
Si 2p	100.5	28.40	28.45	29.00	**28.62**	**0.33**
B 1s	190.0	5.07	4.55	3.97	**4.53**	**0.55**
C 1s	282.5	6.60	0.29	0.28	**2.39**	**3.65**
K 2p	290.5	1.48	6.43	5.86	**4.59**	**2.71**
N 1s	399.0	1.27	1.44	1.28	**1.33**	**0.10**
Ti 2p	457.0	0.61	1.35	1.02	**0.99**	**0.37**
O 1s	529.5	55.84	0.69	0.66	**19.06**	**31.85**
Zn 2p	1019.5	0.28	56.24	57.44	**37.99**	**32.66**
Na 1s	1069.5	0.46	0.55	0.48	**0.50**	**0.05**

XPS Wide Scan Spectrum of ppAA

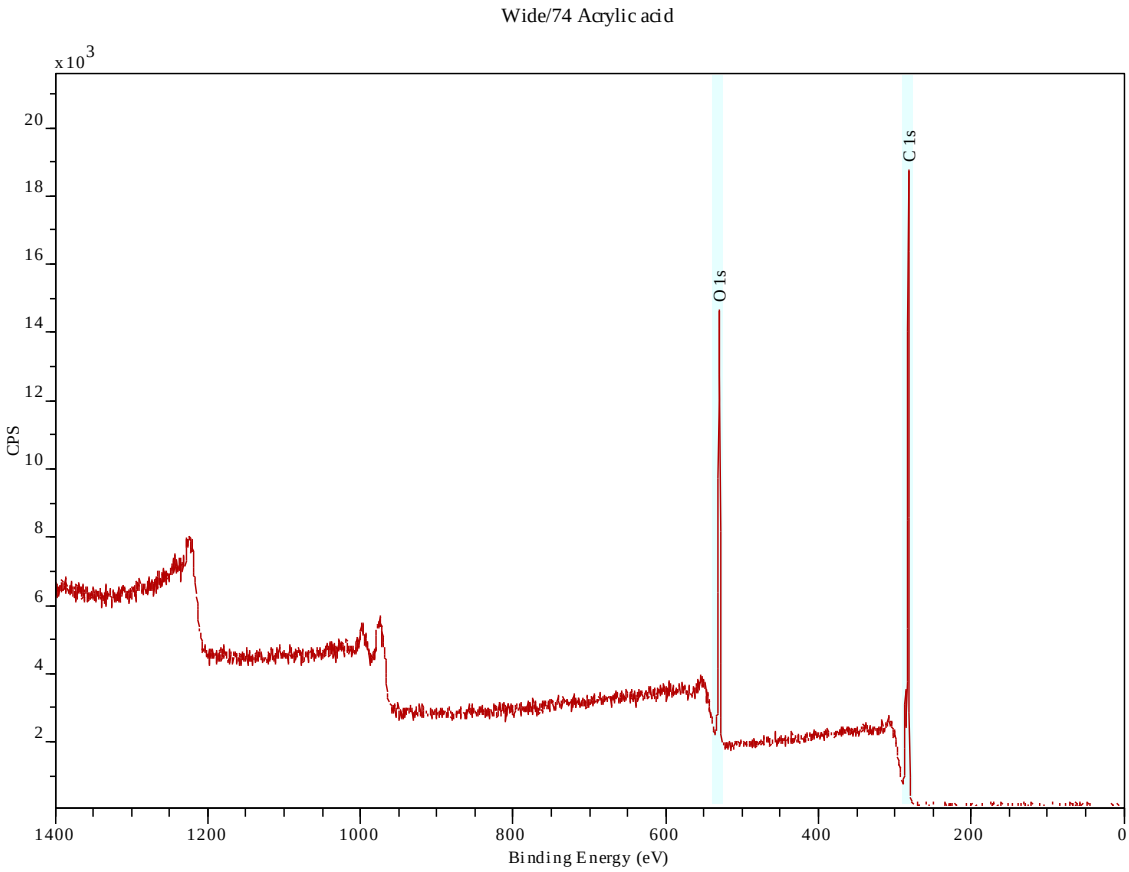

Data of Wide Scans of ppAA

Electrons of Atoms Detected	Binding Energy	Atomic Percentage				
		ppAA Wide Scan 1	PpAA Wide Scan 2	ppAA Wide Scan 3	Average of ppAA Wide Scans	Standard Deviation (+/-)
C 1s	282.0	80.48	80.65	80.85	**80.66**	**0.19**
O 1s	529.5	19.52	19.35	19.15	**19.34**	**0.19**

The O/C ratio is 0.24.

High Resolution XPS Spectrum C1s of ppAA

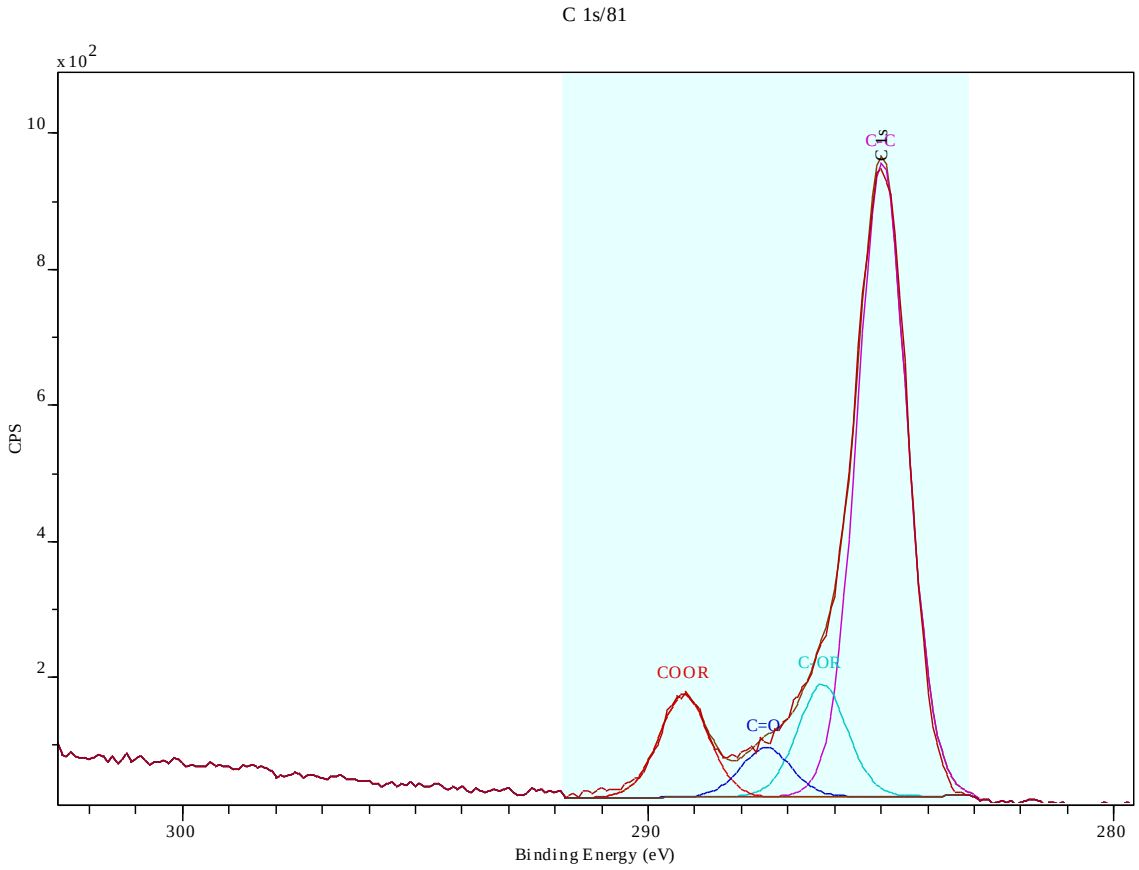

Data of High Resolution XPS Spectrum C1s of ppAA

Electrons of Atoms Detected	Binding Energy	FWHM	Atomic Percentage				
			ppAAm C1s Scan 1	ppAAm C1s Scan 2	ppAAm C1s Scan 3	Average of ppAAm C1s Scans	Standard Deviation (+/-)
C-C	284.9	1.23	70.51	71.64	70.2	**70.78**	**0.76**
C-OR	286.1	1.23	12.50	12.35	11.87	**12.24**	**0.33**
C=O	287.3	1.23	5.544	4.945	7.144	**5.88**	**1.14**
COOR	289.2	1.23	11.44	11.07	10.79	**11.10**	**0.33**

XPS Wide Scan Spectrum of ppAAm

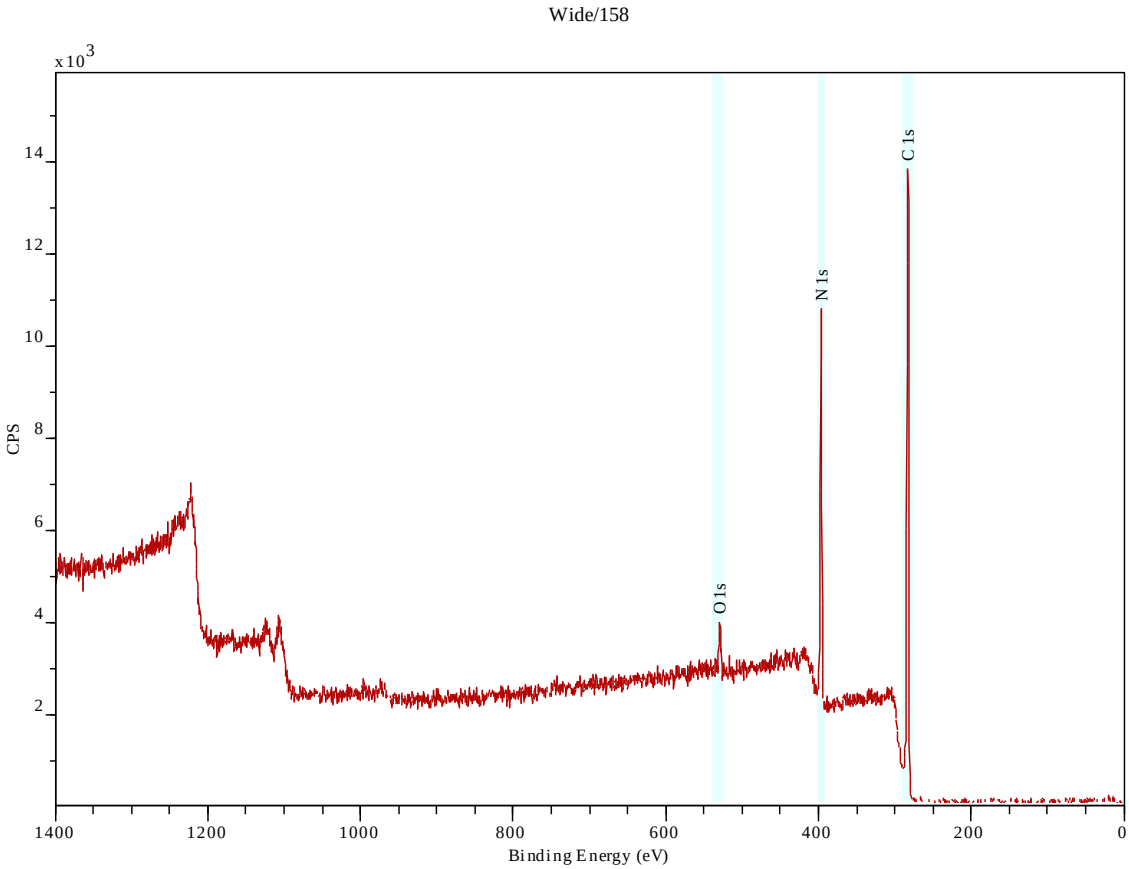

Data of Wide Scans of ppAAm

Electrons of Atoms Detected	Binding Energy	Atomic Percentage				
		ppAAm Wide Scan 1	ppAA Wide Scan 2	ppAAm Wide Scan 3	Average of ppAAm Wide Scans	Standard Deviation (+/-)
C 1s	282.5	77.80	78.88	78.76	**78.48**	**0.59**
N 1s	396.5	19.69	19.29	19.26	**19.41**	**0.24**
O 1s	529.5	2.51	1.83	1.98	**2.11**	**0.36**

The O/C ratio is 0.03.
The N/C ratio is 0.25.

High Resolution XPS Spectrum C1s of ppAAm

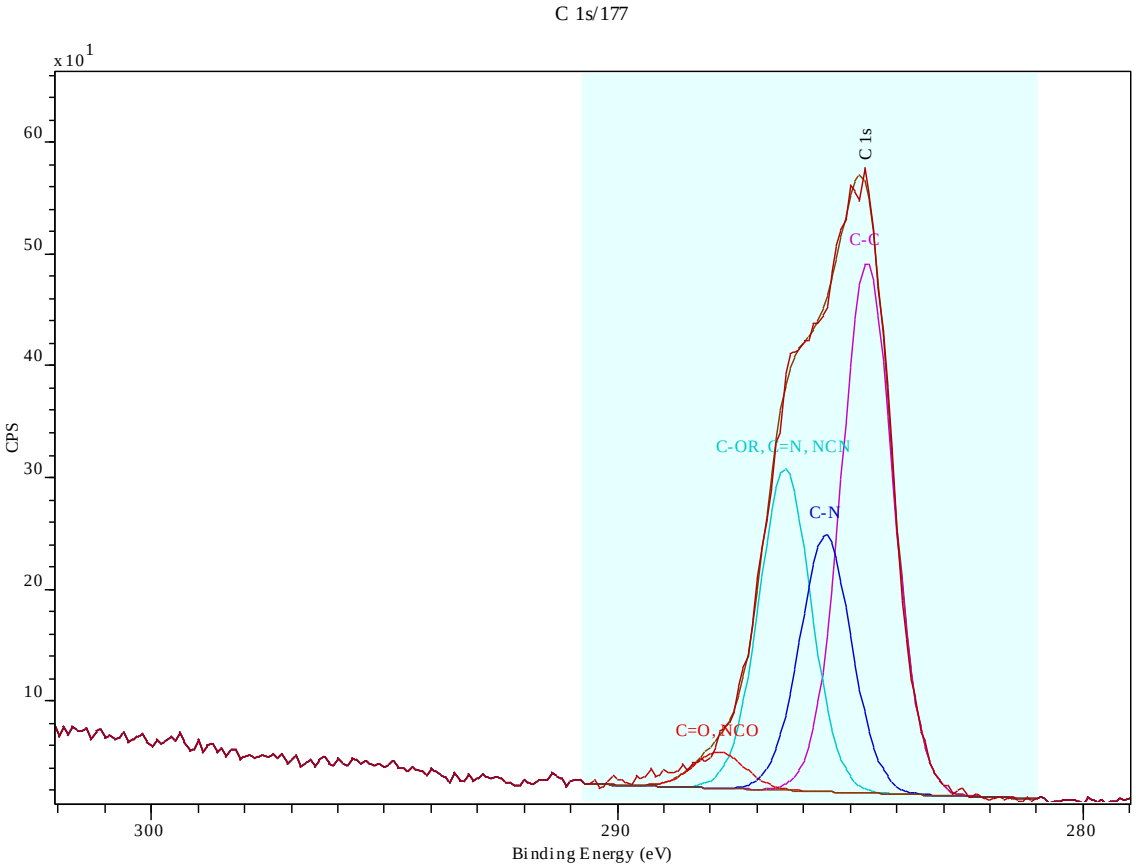

Data of High Resolution XPS Spectrum C1s of ppAAm

Electrons of Atoms Detected	Binding Energy	FWHM	Atomic Percentage				
			ppAAm C1s Scan 1	ppAAm C1s Scan 2	ppAAm C1s Scan 3	Average of ppAAm C1s Scans	Standard Deviation (+/-)
C-C	284.7	1.27	48.13	49.96	46.31	**48.13**	**1.83**
C-N	285.7	1.27	20.03	22.36	22.43	**21.61**	**1.37**
C-OR, C=N, NCN	286.5	1.27	28.68	24.76	28.09	**27.18**	**2.11**
C=O, NCO	287.9	1.27	3.16	2.91	3.17	**3.08**	**0.14**

XPS Wide Scan Spectrum of ppAOH

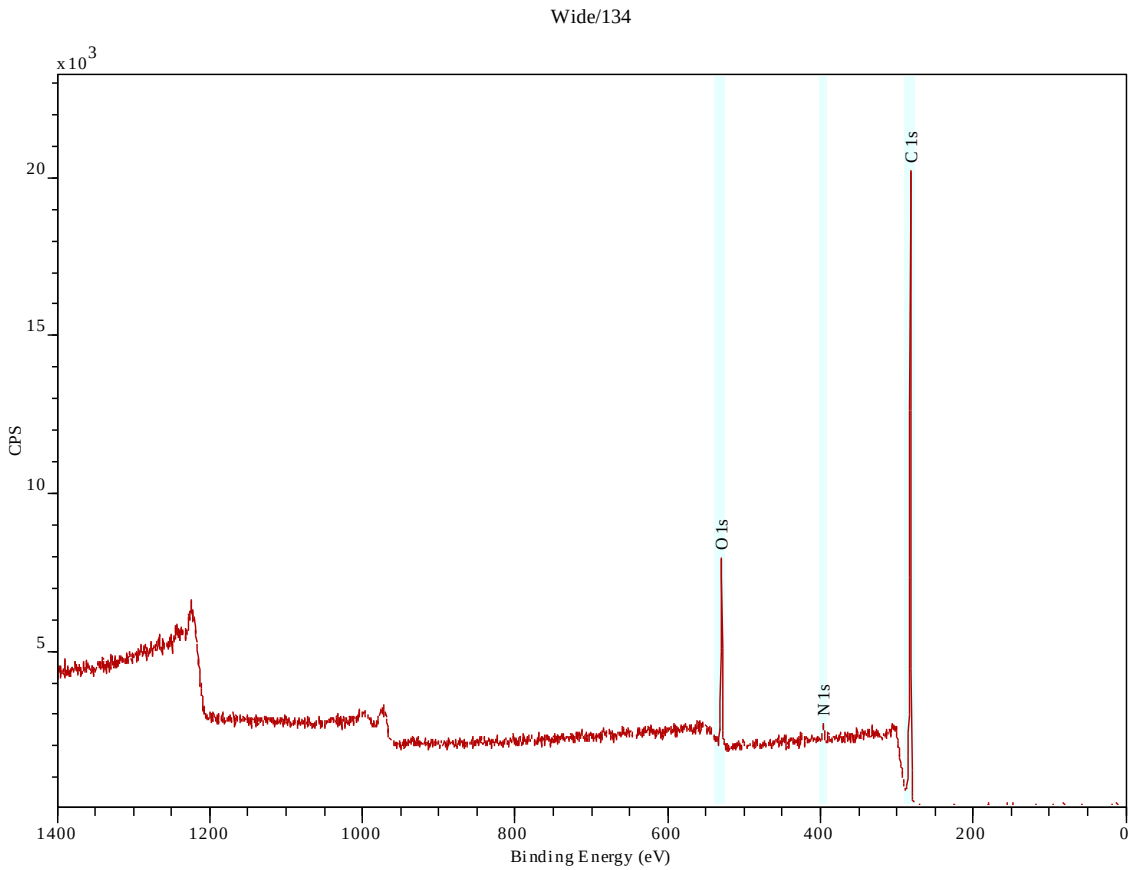

Data of Wide Scans of ppAOH

Electrons of Atoms Detected	Binding Energy	Atomic Percentage				
		ppAOH Wide Scan 1	ppAOH Wide Scan 2	ppAOH Wide Scan 3	Average of ppAOH Wide Scans	Standard Deviation (+/-)
C 1s	281.5	88.81	90.04	89.48	**89.44**	**0.62**
N 1s	396.0	2.43	1.97	2.16	**2.19**	**0.23**
O 1s	529.5	8.75	8.00	8.36	**8.37**	**0.38**

The O/C ratio is 0.09.
The N/C ratio is 0.02.

High Resolution XPS Spectrum C1s of ppAOH

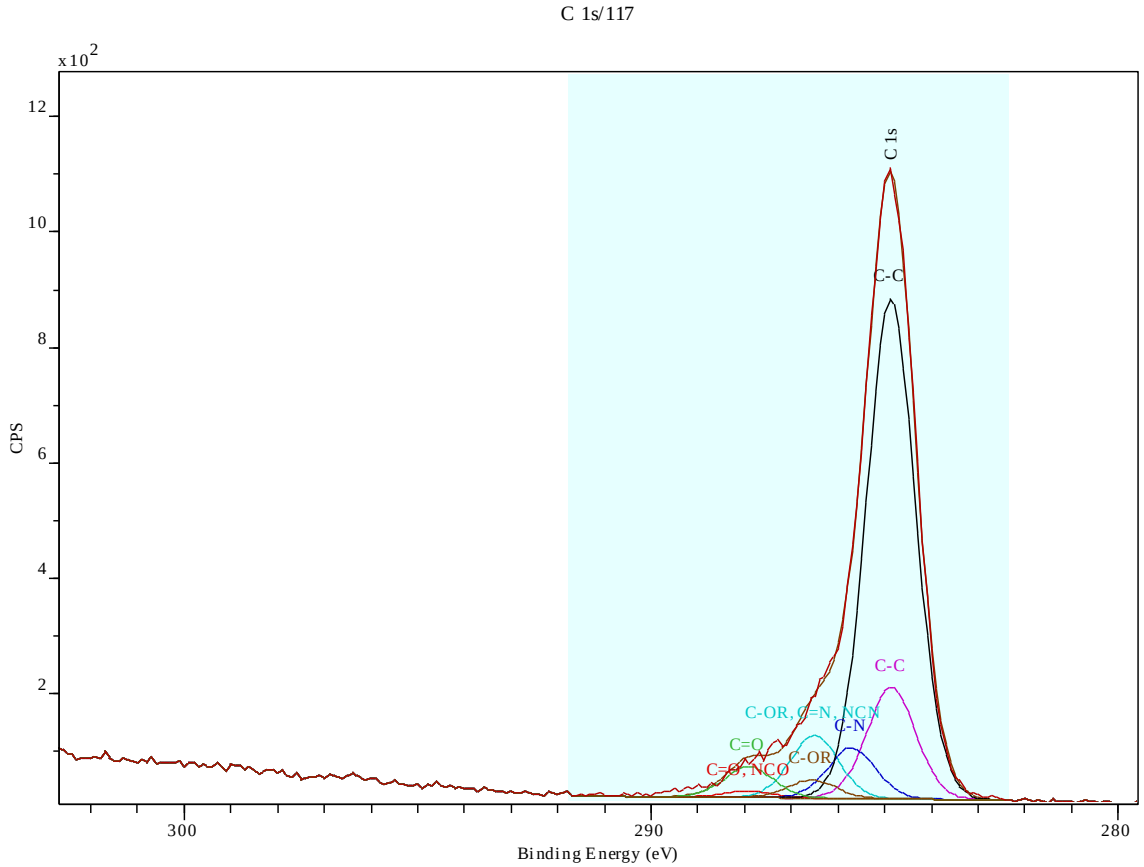

Data of High Resolution XPS Spectrum C1s of ppAOH

Electrons of Atoms Detected	Binding Energy	FWHM	Atomic Percentage				
			ppAOH C1s Scan 1	ppAOH C1s Scan 2	ppAOH C1s Scan 3	Average of ppAOH C1s Scans	Standard Deviation (+/-)
C-C	284.9	1.20	14.32	15.71	17.52	**15.85**	**1.60**
C-C	284.9	1.20	64.09	61.44	59.64	**61.72**	**2.24**
C-N	285.7	1.20	6.44	7.07	7.88	**7.13**	**0.72**
C-OR, C=N, NCN	286.5	1.20	8.02	8.80	9.81	**8.87**	**0.90**
C-OR	286.6	1.20	2.33	2.29	0.88	**1.83**	**0.83**
C=O, NCO	287.9	1.20	0.86	0.94	1.05	**0.95**	**0.10**
C=O	287.9	1.20	3.95	3.74	3.22	**3.64**	**0.38**

Data in red correspond to components of plasma polymerised allylamine contamination.